

Bayesian Inference General Procedures for A Single-subject Test Study

Jie Li^{*1,2}, Gary Green^{2,3}, Sarah J. A. Carr², Peng Liu¹, and Jian Zhang¹

¹School of Mathematics, Statistics and Actuarial Science, University of Kent, Canterbury, CT2 7NF, UK

²Innovision IP Ltd., D5 Culham Science Centre, Oxfordshire, OX14 3DB, UK

³York Neuroimaging Centre, University of York, YO10 5NY, UK

August 29, 2024

Abstract

Abnormality detection in the identification of a single-subject which deviates from the majority of the dataset that comes from a control group is a critical problem. A common approach is to assume that the control group can be characterised in terms of standard Normal statistics and the detection of single abnormal subject is in that context. But in many situations the control group can not be described in terms of Gaussian statistics and the use of standard statistics is inappropriate.

One example of such abnormality detection lies in the detection of traumatic brain injury, which is a particularly common problem, with over 2.8 million individuals a year in America presenting at a Emergency room, (Taylor et al. (2017)). In this article we describe the statistical issues involved in the comparison of a single individual with a large normal control group. We exemplify the use of skewed Student's T statistics to the study of brain activity as a potential biomarker for the identification of a brain injury. We use magnetoencephalography (MEG) as the technology for measuring brain activity and compare single individuals to normal controls from age and gender-matched cohorts.

Existing literature normally assumes that the dataset from the control group follows a normal distribution. However, extensive practical evidence shows that the naive normal distribution assumption is often violated. This violation is frequently observed in brain Magnetoencephalography (MEG) datasets. Therefore, the current approaches using Normal statistics could not be directly applied. Unlike the existing literature, we assume that the dataset from the control group belongs to a more general distributional family - the skewed Student's t distribution, which includes normal distribution and Student's t as a special case. The benefit of this skewed Student's t distributional assumption is that it could cover a variety of empirical behaviours and is thus more suitable for practical needs. This generalisation is essential since many brain Magnetoencephalography (MEG) datasets show a significant level of asymmetry in the observation distribution and hence are highly skewed. It is also the case that the high skewness not only appears in a MEG dataset, but also in other fields, such as cybersecurity, medicine, and neuroscience to name only a few. This paper presents a Bayesian Inference General Procedures for A Single-Subject Test

*Addresses for correspondence: Jie Li, School of Mathematics, Statistics and Actuarial Science, University of Kent, Canterbury CT2 7NF. **Email:** jl725@kent.ac.uk

(BIGPAST), designed to mitigate the effects of skewness. BIGPAST operates under the null hypothesis that the single-subject follows the same distribution as the control group. We assess BIGPAST’s performance against other methods through a series of simulation studies. The results demonstrate that BIGPAST is robust against deviations from normality and outperforms the existing approaches in terms of accuracy. This is because BIGPAST can effectively reduce model misspecification errors under the skewed Student’s t assumption. We apply BIGPAST to a MEG dataset consisting of an individual with mild traumatic brain injury and an age and gender-matched control group, demonstrating its effectiveness in detecting abnormalities in the single-subject.

Keywords— Bayesian inference, Skewed Student’s t distribution, Single-subject test, Control group, Magnetoencephalography (MEG), Jeffery’s prior, and False discovery rate

1 Introduction

Comparing a single-subject against a control group is a fundamental task in many scientific fields, including medicine, psychology, and neuroscience (Scholz and Stephens, 1987; Crawford and Howell, 1998; Crawford and Garthwaite, 2007). The control group’s distribution is typically assumed to follow a normal distribution. Under this assumption, there exist several methods that are able to compare a single-subject against a control group. Crawford and Howell (1998) proposed a t -score defined as follows:

$$t = \frac{x^* - \bar{x}}{s/\sqrt{(n+1)/n}},$$

where x^* represents the observation of the single-subject, \bar{x} denotes the average of the control group with n observations, and s stands for the standard deviation of the dataset from a control group. The test score t follows a Student’s t distribution with $n - 1$ degrees of freedom. Let α be the prespecified significant level, if the p value, $\mathbb{P}(t > |t_{1-\alpha/2}(n-1)|)$, is less than α where $t_{1-\alpha/2}(n-1)$ is the $(1 - \alpha/2)$ -th critical value of Student’s t distribution with $n - 1$ degrees of freedom, then one can claim that x^* has an abnormality. However, one potential issue is that the distribution of the data from the control group may not follow the normal distribution, which will violate the assumption and thus the previous methodology from Crawford (1998) will not be valid. In order to amend it, Crawford et al. (2006) examined the effects of departures from normality on testing for a deficit in a single-subject via using a Leptokurtic distribution with different skewness parameters. They asserted that the t score (Crawford and Howell, 1998) outperforms the z score in terms of type I error, and the t score shows robustness as good as the result under the normal assumption. Additionally, Crawford and Garthwaite (2006) investigated the statistical power of testing for an abnormality in a single-subject using Monte Carlo simulations. They claimed that the power of t score performs slightly worse compared with the results under normal assumption.

The simulation results for type I error in Crawford et al. (2006) and power Crawford and Garthwaite (2006) led to the assertion that the t score (Crawford and Howell, 1998) is robust even when the underlying distribution is skewed Student’s t distribution. However, the simulation settings in Crawford et al. (2006) and Crawford and Garthwaite (2006) are not comprehensive (ground true observations of a single subject are not well-mixed) to evaluate the performance of t score under skewed Student’s t distribution. For instance, in evaluating type I error, Crawford et al. (2006) generates all single-subject observations from the distribution of the control group. Conversely, for the power analysis in Crawford and Garthwaite (2006) all single-subject observations are generated from a distribution that is different from the distribution of control group. The above authors only consider two special parameter settings of single-subject, if 50%

of the single-subject observations are generated from distribution of the control group, the other 50% of observation comes from a different distribution, the type I error and power of the t score test would differ significantly, for example the powers (in median) of Crawford-Garthwaite (CG) method and BIGPAST under two-sided test are around 0.62 and 0.96 respectively, as illustrated in [Figure 1c](#).

One reason that the skewed Student's t distribution assumption performs better than the normal distribution assumption lies in the fact that the skewness of the skewed Student's t distribution affects the lower and upper tails, and in turn, the type I error and power of the t score test. The skewness changes the symmetry, and as a consequence, the skewed Student's t distribution has one lighter tail and one heavier tail. When the skewness is positive, the upper tail of the skewed Student's t distribution becomes heavier, while the lower tail becomes lighter. For negative skewness, the lower tail is heavier while the upper tail is lighter, see [Figure 2](#). In the parameter settings of [Crawford et al. \(2006\)](#); [Crawford and Garthwaite \(2006\)](#), the skewness is negative, i.e., the lower tail is a heavier tail. They only consider that the direction of alternative hypothesis is 'less' which means that for the same significance level, the critical value of skewed Student's t distribution is smaller than the critical value of Student's t distribution. It implies that without considering the randomness, if x^* is claimed as abnormal by critical value of skewed Student's t distribution, then x^* must be claimed as abnormal by t score test. Furthermore, because all single-subject observations are generated from the distribution of the control group in [Crawford et al. \(2006\)](#), the true positive rate is undefined. By combination of above settings, [Crawford et al. \(2006\)](#) claimed that the t score is robust even under skewed Student's t distribution. However, it is only true for the specific settings in [Crawford et al. \(2006\)](#). If one of the direction of alternative hypothesis, the sign of skewness or the data generation mechanism of single-subject observations changes, then the performance of t score test is different. For example, the type I error of t score test under two-sided test when $n = 400$ is up to 0.1215, while the true positive rate of BIGPAST is just 0.0187 as displayed in [Table 3](#). The difference implies that t score test is not suitable for abnormality detection under skewed Student's t distribution. For the power analysis, as outlined by [Crawford et al. \(2006\)](#), we can employ the aforementioned procedures, bearing in mind that all observations of the single-subject are positive. For a more detailed discussion, please refer to the simulation study in [Section 3.2](#).

Hence, the interplay between skewness (whether positive or negative), the type of hypothesis ('two-sided', 'less', or 'greater'), and the method of generating the single-subject observation significantly influences both the type I error rate and the power of the t score test under the assumption of skewed Student's t distribution. Under this assumption, neither the z score test, the t score test, nor even the Crawford-Garthwaite Bayesian method ([Crawford and Garthwaite, 2007](#)) can eliminate the model misspecification error. To be specific, we investigate the model misspecification error between normal and skewed Student's t distributions in [Figure 2](#). The regions shaded in light-red colour in [Figures 2a](#) and [2b](#) represent the model misspecification errors that occur when the skewed Student's t distribution is assumed, but the z score test is used. Apparently, the z score will always be affected by model misspecification error under the skewed Student's t distribution assumptions.

The rationale for this paper's assumption of the skewed Student's t distribution can be attributed to two key factors. On one hand, the concept of skewness has become increasingly significant in the fields of statistics and neuroscience ([Azzalini and Capitanio, 2003](#); [Crawford and Garthwaite, 2006](#); [Buzsáki and Mizuseki, 2014](#)). As a result, the skewed Student's t distribution ([Azzalini and Capitanio, 2014](#)) has obtained considerable attention ([Ismail et al., 2013](#)). On the other hand, assuming a skewed Student's t distribution can help eliminate model misspecification errors, provided that the underlying distribution is a special case of the skewed Student's t distribution. These special cases encompass the Student's t distribution, half Stu-

dent's t distribution, skew normal distribution, half normal distribution, Cauchy distribution, half Cauchy distribution, and skew Cauchy distribution. To show this, simulation results with normal assumption but using BIGPAST method can be found in [Table 8](#).

This paper introduces a Bayesian Inference General Procedures for A Single-subject Test (BIGPAST) framework. The BIGPAST framework parallels the Bayesian inference framework of Crawford-Garthwaite ([Crawford and Garthwaite, 2007](#)), with the critical difference being our assumption of the skewed Student's t distribution. As the skewed Student's t distribution is a generalisation of both the Student's t and skewed normal distributions, the BIGPAST is equivalent to the Bayesian inference framework of Crawford-Gathwaite ([Crawford and Garthwaite, 2007](#)) under the assumption of a normal distribution. Additionally, we propose a Jeffery's prior, defined by explicit mathematical formulas. We evaluate BIGPAST's performance against the existing approaches through simulation studies. The results demonstrate that BIGPAST is robust against departures from normality and surpasses the existing methods based on the assumption of a normal distribution in terms of type I error, power and accuracy.

The remainder of the paper is organised as follows. In [Section 2](#), we introduce the Bayesian inference procedures for comparing a single-subject with a control group under the skewed Student's t distribution. In [Section 3](#), we conduct a comprehensive set of simulation studies to evaluate the performance of the proposed BIGPAST method. We then apply the BIGPAST method to a MEG dataset comprising an individual with mild traumatic brain injury and a control group in [Section 4](#). Finally, we summarise our findings and discuss future research directions in [Section 5](#).

2 Bayesian Inference Procedures for Single-subject's Abnormality Detection

In this section, we introduce a Bayesian inference procedures to compare a single-subject with a control group, under the assumption that the control group follows a skewed Student's t distribution. For practical applications, we recommend employing a modified version of the general goodness-of-fit test ([Chen and Balakrishnan, 1995](#)) tailored explicitly for the skewed Student's t distribution.

2.1 Goodness-of-fit for Skewed Student's t Distribution

To test the null hypothesis $H_0 : x_1, x_2, \dots, x_n$ as a random sample from the skewed Student's t distribution, the definition of skewed Student's t distribution can be found in [Section 2.3](#). We denote $F(x|\alpha, \nu, \xi, \omega)$ as the cumulative function of this distribution where The parameters α, ν, ξ, ω are unknown. The following steps outline the testing process:

- (a) Estimate the parameters $\hat{\alpha}, \hat{\nu}, \hat{\xi}, \hat{\omega}$ by maximising the likelihood function.
- (b) Compute the empirical distribution function $v_i = F(x|\hat{\alpha}, \hat{\nu}, \hat{\xi}, \hat{\omega})$ for $i = 1, 2, \dots, n$.
- (c) Compute $y_i = \Phi^{-1}(v_i)$, where Φ is the standard normal cumulative distribution function.
- (d) Let $u_i = \Phi((y_i - \bar{y})/s_y)$, where $\bar{y} = n^{-1} \sum_{i=1}^n y_i$ and $s_y^2 = (n-1)^{-1} \sum_{i=1}^n (y_i - \bar{y})^2$. Let $u_{(1)}, \dots, u_{(n)}$ be the order statistics of u_1, \dots, u_n .
- (e) Calculate the Anderson statistic A^2 based on $u_{(1)}, \dots, u_{(n)}$, i.e.,

$$A^2 := -n - n^{-1} \sum_{i=1}^n [(2i-1) \log(u_{(i)}) + (2n+1-2i) \log(1-u_{(i)})].$$

Modify A^2 into $A^* := A^2(1 + 0.75/n + 2.25/n^2)$. If A^* exceeds the critical value at a given significance level, reject H_0 .

More details on the testing procedures and critical points can be found in [Chen and Balakrishnan \(1995\)](#).

If the null hypothesis H_0 is accepted at some significance level, we can proceed with the comparison procedures between a single-subject and the control group described in the next section. If H_0 is rejected, a non-parametric method can be implemented to compare a single-subject with the control group. While the discussion of the non-parametric method is beyond the scope of this paper, we plan to extend this approach in future work. Notably, the skewed Student's t distribution encompasses the regular Student's t distribution ($\alpha = 0$), skewed normal distribution ($\nu = \infty$), half normal distribution ($\alpha = \pm\infty, \nu = \infty$), and normal distribution ($\alpha = 0, \nu = \infty$) as special cases. For simplicity, we assume that the control group data follows a skewed Student's t distribution in the subsequent sections. The advantage of this assumption is that the BIGPAST method performs comparably to the Crawford-Garthwaite methods ([Crawford and Howell, 1998](#); [Crawford and Garthwaite, 2007](#)) when the control group data adheres to a normal distribution, as demonstrated in [Table 8](#).

2.2 Bayesian Inference General Procedures for a Single-subject Test (BIGPAST)

Consider a control group with observations x_1, x_2, \dots, x_n , assumed to follow a skewed Student's t distribution with unknown parameters α, ν, ξ, ω . Let x^* denote the observation of a single-subject. Our goal is to test whether x^* is a random sample from the same distribution as the control group. Let $f_c(\alpha, \nu, \xi, \omega)$ represent the skewed Student's t density function of the control group's observations. The hypothesis testing can be formulated as follows:

$$\mathcal{H}_0 : x^* \sim f_c(\alpha, \nu, \xi, \omega) \quad v.s. \quad \mathcal{H}_1 : x^* \not\sim f_c(\alpha, \nu, \xi, \omega),$$

where $\not\sim$ represents that x^* is not a random sample from $f_c(\alpha, \nu, \xi, \omega)$. We propose the Bayesian inference general procedures for a single-subject test under the null hypothesis \mathcal{H}_0 . The procedures are as follows:

1. Choose the proposed Jeffery prior $\pi^J(\alpha, \nu, \xi, \omega)$ as the joint prior of α, ν, ξ, ω .
2. Compute the posterior distribution of α, ν, ξ, ω based on the control group observations $\mathbf{x} = (x_1, x_2, \dots, x_n)$ and the prior $\pi^J(\alpha, \nu, \xi, \omega)$. By Bayes's Theorem, we have

$$\pi(\alpha, \nu, \xi, \omega | \mathbf{x}) \propto l(\mathbf{x} | \alpha, \nu, \xi, \omega) \pi^J(\alpha, \nu, \xi, \omega),$$

where $l(\mathbf{x} | \alpha, \nu, \xi, \omega) := \prod_{i=1}^n f_c(x_i | \alpha, \nu, \xi, \omega)$ is the likelihood function.

3. Draw m samples of α, ν, ξ, ω from the posterior distribution $\pi(\alpha, \nu, \xi, \omega | \mathbf{x})$ by Metropolis-Hastings algorithm ([Hastings, 1970](#)) with normal proposal, denoted as $\alpha_j, \nu_j, \xi_j, \omega_j, j = 1, 2, \dots, m$.
4. For each $\alpha_j, \nu_j, \xi_j, \omega_j$, draw s random samples from the skewed Student's t distribution with parameters $\alpha_j, \nu_j, \xi_j, \omega_j$, denoted as $x_{1j}, x_{2j}, \dots, x_{sj}, j = 1, 2, \dots, m$. Sort the observations $x_{1j}, x_{2j}, \dots, x_{sj}, j = 1, 2, \dots, m$, in ascending order and label them as $x_{(1)}, x_{(2)}, \dots, x_{(B)}$ where $B = ms$.
5. Given the significance level α^* and \mathbf{x} , the credible interval of x^* is $[x_{(\lfloor B\alpha^*/2 \rfloor)}, x_{(\lceil B(1-\alpha^*/2) \rceil)}]$, where $\lfloor \cdot \rfloor$ and $\lceil \cdot \rceil$ are the floor and ceiling functions, respectively. If x^* is not in the credible interval, then reject the null hypothesis \mathcal{H}_0 at the significance level α^* .

Remarks When $\alpha \rightarrow +\infty$ or $-\infty$, the skewed Student's t distribution degenerates to half Student's t distribution. Therefore, the two-sided credible interval in Step 5 above could be $[x_{(1)}, x_{(\lceil B(1-\alpha^*) \rceil)}]$ if $\alpha = +\infty$ or $[x_{(\lfloor B\alpha^* \rfloor)}, x_{(B)}]$ if $\alpha = -\infty$. BIGPAST is similar to the Bayesian inference framework of Crawford-Garthwaite (Crawford and Garthwaite, 2007) except that they employed a tail probability based on the assumption of normal distribution. Furthermore, procedures 1-3 above can be extended to other distributions, provided that a prior can be assigned for a specific density distribution.

2.3 Jeffery's Priors

In Bayesian probability, the Jeffreys prior (Jeffreys, 1946) refers to a prior density function that is proportional to the square root of the determinant of the Fisher information matrix. In this section, we proposed an explicit Jeffery prior for the parameters of skewed Student's t distribution and compare it to the existing priors.

Let $f(z|\alpha, \nu)$ be the non-linear skewed Student's t density function (Azzalini and Capitanio, 2003), defined as follows:

$$f(z|\alpha, \nu) := 2t(z|\nu)T(w|\nu + 1), \quad z \in \mathbb{R}, \alpha \in \mathbb{R}, \nu > 0,$$

where $r(z, \nu) = \sqrt{(\nu + 1)/(\nu + z^2)}$ and $w = \alpha z r(z, \nu)$, $t(\cdot|\nu)$ represents the density function of t distribution with degree of freedom ν , and $T(\cdot|\nu + 1)$ represents the cumulative density function of t distribution with degree of freedom $\nu + 1$. Let ξ and ω be the location and scale parameters, then the skewed Student's t density function is given by

$$f(x|\alpha, \nu, \xi, \omega) := \frac{1}{\omega} f\left(\frac{x - \xi}{\omega} | \alpha, \nu\right).$$

In the literature, two types of priors are commonly used for ξ and ω : the partial information prior (Sun and Berger, 1998) and the independence Jeffery's prior (Rubio and Steel, 2014). Both of these priors assume that the joint prior of ξ and ω , denoted as $\pi(\xi, \omega)$, is proportional to ω^{-1} . Consequently, the joint prior of α, ν, ξ, ω can be expressed as follows:

$$\pi(\alpha, \nu, \xi, \omega) \propto \omega^{-1} \pi(\alpha, \nu).$$

The joint prior of α and ν , $\pi(\alpha, \nu)$, may be specified by the Jeffery's prior (Branco et al., 2013) or the natural informative prior (Dette et al., 2018). Branco et al. (2013) proposed the following prior for general non-linear skewed Student's t density function:

$$\pi^B(\alpha, \nu, \xi, \omega) \propto \omega^{-1} (8\alpha^2 + \pi^2)^{-3/4} \pi(\nu),$$

where $\pi(\nu)$ is proposed by Fonseca et al. (2008) for the Student's t distribution and given by

$$\pi(\nu) \propto \left(\frac{\nu}{\nu + 3}\right)^{1/2} \left\{ \psi^{(1)}\left(\frac{\nu}{2}\right) - \psi^{(1)}\left(\frac{\nu + 1}{2}\right) - \frac{2(\nu + 3)}{\nu(\nu + 1)^2} \right\}^{1/2},$$

where $\psi^{(1)}(\cdot)$ is the trigamma function, i.e., the second derivative of $\log(\Gamma(\cdot))$. Here, $\Gamma(\cdot)$ is the Gamma function. When $\alpha \rightarrow +\infty$, the order of $\pi^B(\alpha, \nu, \xi, \omega)$ with respect to α is $O(\alpha^{-3/2})$ (Branco et al., 2013).

Dette et al. (2018) proposed the so-called natural informative prior of the parameter α based on the total variance distance, which is given by

$$BTV(\alpha|\theta_1, \theta_2) = \frac{1}{B(\theta_1, \theta_2)} \left(\frac{\tan^{-1}(\alpha)}{\pi} + \frac{1}{2}\right)^{\theta_1 - 1} \left(\frac{-\tan^{-1}(\alpha)}{\pi} + \frac{1}{2}\right)^{\theta_2 - 1} \frac{1}{\pi(1 + \alpha^2)},$$

where $B(\cdot, \cdot)$ represents the Beta function. When $\theta_1 = 1, \theta_2 = 1$, the prior $BTV(\alpha|1, 1)$ reduces to the standard Cauchy prior. Similarly, [Dette et al. \(2018\)](#) constructed the joint prior of α, ν, ξ, ω based on $BTV(\alpha|1, 1)$ as

$$\boldsymbol{\pi}^D(\alpha, \nu, \xi, \omega) \propto \omega^{-1} \pi^{-1} (1 + \alpha^2)^{-1} \boldsymbol{\pi}(\nu),$$

which is order of $O(\alpha^{-2})$ when $\alpha \rightarrow +\infty$.

A notable concern with $\boldsymbol{\pi}^B(\alpha, \nu, \xi, \omega)$ and $\boldsymbol{\pi}^D(\alpha, \nu, \xi, \omega)$ is that the marginal prior of ν is independent of α . However, given that the skewed Student's t distribution is a generalisation of the Student's t distribution, the marginal prior of ν should ideally depend on α . To address this issue, we propose the Jeffery's prior for the skewed Student's t density function, as detailed in [Theorem 2.1](#).

Theorem 2.1. *Let $f(z|\alpha, \nu)$ be the non-linear skewed Student's t density function, defined as follows:*

$$f(z|\alpha, \nu) := 2t(z|\nu)T(w|\nu + 1), \quad z \in \mathbb{R}, \alpha \in \mathbb{R}, \nu > 0,$$

where $r(z, \nu) = \sqrt{(\nu + 1)/(\nu + z^2)}$ and $w = \alpha z r(z, \nu)$. Given any $\nu > 0$, let $\boldsymbol{\pi}^J(\alpha, \nu)$ represent the joint Jeffery's prior for α and ν , we have

$$\boldsymbol{\pi}^J(\alpha, \nu) \propto \sqrt{I_{\alpha\alpha} I_{\nu\nu} - I_{\alpha\nu}^2}, \quad (1)$$

and the joint prior of α, ν, ξ, ω is given by

$$\boldsymbol{\pi}^J(\alpha, \nu, \xi, \omega) \propto \omega^{-1} \boldsymbol{\pi}^J(\alpha, \nu), \quad (2)$$

where

$$\begin{aligned} I_{\nu\nu} &= \mathbb{E} \left[h^2(w) \frac{\alpha^2 z^2 (\nu + 1)}{4(\nu + z^2)^3} \right] + \frac{1}{4} \mathbb{E} \left[\left(\log \frac{\nu}{\nu + z^2} \right)^2 \right] + \frac{1}{4} \mathbb{E} \left[\left(\frac{z^2 - 1}{\nu + z^2} \right)^2 \right] + d_\nu^2 \\ &\quad + \frac{1}{2} \mathbb{E} \left[\left(\log \frac{\nu}{\nu + z^2} \right) \left(\frac{z^2 - 1}{\nu + z^2} \right) \right] + d_\nu \mathbb{E} \left[\log \frac{\nu}{\nu + z^2} \right] \\ I_{\alpha\nu} &= - \frac{\pi \alpha \Gamma \left(\frac{\nu}{2} + 1 \right)^2 \left((\nu + 4) H_5 - \frac{(\alpha^2 (2\nu + 3) + (\nu + 3) \sigma_{\nu+1}^2) H_6}{\sigma_{\nu+1}^2} \right)}{8(\alpha^2 + \sigma_{\nu+1}^2) \Gamma \left(\frac{\nu+1}{2} \right) \Gamma \left(\frac{\nu+5}{2} \right)}, \end{aligned}$$

and

$$\begin{aligned} \mathbb{E} \left[\log \frac{\nu}{\nu + z^2} \right] &= \psi \left(\frac{\nu}{2} \right) - \psi \left(\frac{\nu + 1}{2} \right) \\ \mathbb{E} \left[\left(\log \frac{\nu}{\nu + z^2} \right) \left(\frac{z^2 - 1}{\nu + z^2} \right) \right] &= - \frac{1}{\nu^2 + \nu} \\ \mathbb{E} \left[\left(\frac{z^2 - 1}{\nu + z^2} \right)^2 \right] &= \frac{1}{\nu^2 + 3\nu} \\ \mathbb{E} \left[\left(\log \frac{\nu}{\nu + z^2} \right)^2 \right] &= \left(\psi \left(\frac{\nu}{2} \right) - \psi \left(\frac{\nu + 1}{2} \right) \right)^2 + \psi^{(1)} \left(\frac{\nu}{2} \right) - \psi^{(1)} \left(\frac{\nu + 1}{2} \right) \\ \mathbb{E} \left[h^2(w) \frac{\alpha^2 z^2 (\nu + 1)}{4(\nu + z^2)^3} \right] &= \frac{\pi^{5/2} \Gamma \left(\frac{\nu}{2} + 1 \right) ((\nu + 3) H_1 - (\nu + 3) H_2 - H_3 + H_4)}{8\nu^2 \Gamma \left(\frac{\nu+5}{2} \right) B \left(\frac{\nu}{2}, \frac{1}{2} \right) B \left(\frac{\nu+1}{2}, \frac{1}{2} \right)^2}. \end{aligned}$$

Furthermore, we define $d_\nu := -\frac{1}{2}\psi\left(\frac{\nu}{2}\right) + \frac{1}{2}\psi\left(\frac{\nu+2}{2}\right) + 2c_\nu * g_1(\nu)$, where c_ν is a constant that depends solely on ν . The hypergeometric functions, denoted as $H_1, H_2, H_3, H_4, H_5, H_6$, along with $h^2(w)$ and $g_1(\nu)$ are defined in the proof. The term $\sigma_{\nu+1}^2$ is defined in [Lemma A.1](#). The functions $\psi(\cdot)$ and $\psi^{(1)}(\cdot)$ represent the digamma and trigamma function respectively.

The proof of [Theorem 2.1](#) can be found in Appendix. Upon applying a Taylor expansion, we find that as $\alpha \rightarrow 0$, the order of $\pi^J(\alpha, \nu, \xi, \omega)$ with respect to α is $O(1 + \alpha^2)$. Conversely, as $\alpha \rightarrow +\infty$, the order becomes $O(\alpha^{-3/2})$, aligning with the findings of [Branco et al. \(2013\)](#). The computation of $\pi^J(\alpha, \nu, \xi, \omega)$ relies solely on the basic functions provided by the Python packages *scipy* and *numpy*. As such, the formulas in [Theorem 2.1](#) can be directly implemented to define a function for computing Jeffery’s prior. Additionally, we have developed a Python package, *skewt-scipy* (<https://pypi.org/project/skewt-scipy/>), specifically for the skewed Student’s t distribution.

For the Bayesian estimation of ν , we anticipate that $\pi^J(\alpha, \nu, \xi, \omega)$ will outperform $\pi^B(\alpha, \nu, \xi, \omega)$. Because $\pi^J(\alpha, \nu, \xi, \omega)$ depends on α , unlike $\pi(\nu)$ in $\pi^B(\alpha, \nu, \xi, \omega)$ is independent of α . This is verified by the comparison study in [Section 3](#). The Jeffery’s prior $\pi^J(\alpha, \nu, \xi, \omega)$ is a suitable choice for the skewed Student’s t density function. The BIGPAST based on Jeffery’s prior $\pi^J(\alpha, \nu, \xi, \omega)$ is robust to the departures from normality and outperforms the existing approaches based on the assumption of normal distribution in terms of type I error, power and accuracy.

3 Simulation

3.1 Jeffery’s Prior Comparison Study

In this section, we conduct a comparative analysis of our proposed prior $\pi^J(\alpha, \nu, \xi, \omega)$ against the priors $\pi^B(\alpha, \nu, \xi, \omega)$ and $\pi^D(\alpha, \nu, \xi, \omega)$. We evaluate these priors under six different parameter settings for (α, ν) : $(-1, 1)$, $(-10, 10)$, $(-30, 30)$, $(-50, 50)$, $(-1, 50)$, and $(-50, 1)$. For each setting, the location and scale parameters are fixed at $\xi = -2, \omega = \sqrt{2}$. To simplify the notation, we use π^J, π^B , and π^D as shorthand for $\pi^J(\alpha, \nu, \xi, \omega), \pi^B(\alpha, \nu, \xi, \omega)$, and $\pi^D(\alpha, \nu, \xi, \omega)$, respectively. For each parameter setting, we generate $N = 1000$ samples, each with a sample size of $n = 500$, from the non-linear skewed Student’s t density function. We then numerically minimise the negative logarithm of the posterior distribution to obtain the maximum posterior estimators of α, ν, ξ, ω . The performance of different priors is evaluated using the mean absolute deviation (MAD) from the true parameter. The MAD is calculated as $1/N \sum_{i=1}^N |\hat{\theta}_i - \theta|$, where θ is the true parameter and $\hat{\theta}_i$ is the i -th maximum posterior estimator of θ . Our comparative study also includes the maximum likelihood estimators (MLE). The results are presented in [Table 1](#).

As demonstrated in [Table 1](#), when $|\alpha|$ and ν are less than 30, the performance of π^J aligns closely with that of π^B and π^D in terms of estimating α and ν . However, for larger values of $|\alpha|$ and ν , π^J outperforms both π^B and π^D . Furthermore, π^J, π^B , and π^D all outperform the maximum likelihood estimators (MLE) for larger $|\alpha|$ and ν . In terms of estimating the location ξ and scale ω , the mean absolute deviations (MADs) of all priors are comparable to the MLE. These results underscore the efficacy of π^J for the non-linear skewed Student’s t density function, particularly when $|\alpha|$ and ν exceed 30.

3.2 Comparison with Existing Approaches

To evaluate the performance of BIGPAST in comparison to the z -score, t -score ([Crawford and Howell, 1998](#)), Crawford-Garthwaite Bayesian approach ([Crawford and Garthwaite, 2007](#)), and

Parameters	Priors	(α, ν)					
		$(-1, 1)$	$(-10, 10)$	$(-30, 30)$	$(-50, 50)$	$(-1, 50)$	$(-50, 1)$
α	$\pi^J, c_\nu = 0$	0.156	1.989	9.402	11.839	0.471	8.415
	$\pi^J, c_\nu = 1$	0.162	2.009	9.105	11.072	0.457	7.703
	π^B	0.142	1.901	9.399	14.267	0.497	11.489
	π^D	0.142	1.913	9.122	14.362	0.532	11.807
	Uniform	0.146	2.451	236.974	375.183	0.385	612.510
ν	$\pi^J, c_\nu = 0$	0.079	2.612	6.130	6.656	14.321	0.064
	$\pi^J, c_\nu = 1$	0.085	2.418	5.474	6.210	8.961	0.063
	π^B	0.064	2.642	15.143	20.924	35.187	0.061
	π^D	0.063	2.671	15.247	21.587	35.319	0.061
	Uniform	0.064	13.619	82.848	50.030	27.068	0.062
ξ	$\pi^J, c_\nu = 0$	0.136	0.035	0.017	0.012	0.344	0.017
	$\pi^J, c_\nu = 1$	0.148	0.035	0.016	0.011	0.333	0.013
	π^B	0.104	0.028	0.018	0.013	0.373	0.012
	π^D	0.105	0.029	0.019	0.014	0.401	0.013
	Uniform	0.105	0.026	0.016	0.010	0.261	0.011
ω	$\pi^J, c_\nu = 0$	0.120	0.071	0.049	0.041	0.156	0.088
	$\pi^J, c_\nu = 1$	0.128	0.067	0.046	0.039	0.143	0.085
	π^B	0.099	0.076	0.076	0.064	0.199	0.085
	π^D	0.099	0.078	0.079	0.068	0.211	0.086
	Uniform	0.099	0.070	0.047	0.040	0.109	0.083

Table 1: Comparison of the mean absolute deviation (MAD) among π^J with $c_\nu = 0$ and $c_\nu = 1$, π^B , π^D , and the Uniform prior. The maximum a posteriori (MAP) estimation with a Uniform prior distribution is generally equivalent to the maximum likelihood estimation (MLE). Each entry in the table represents the MAD, calculated based on 1000 replications.

Anderson-Darling non-parametric approach (Scholz and Stephens, 1987) for abnormality detection in a single-subject against a control group, we adopt the skew Settings from Section 3.1.1 in Crawford et al. (2006). The data are generated from the skewed Student’s t distribution with parameters $\alpha = -3.23$, $\nu = 7$, $\xi = 0$, and $\omega = 1$, which correspond to the skew Settings in Section 3 of Crawford et al. (2006). We consider sample sizes of 50, 100, 200, and 400. The single-subject and control group observations are generated from the aforementioned skewed Student’s t distribution. For more mechanisms of data generation, see Crawford and Garthwaite (2006). The code for this simulations in this section can be found in [GitHub repository: BIGPAST](#). With a significance level of 0.05 and a one-sided test (where the direction of the alternative hypothesis is ‘less’), we record the abnormality detection results using the z -score, t -score, Crawford-Garthwaite Bayesian method, Anderson-Darling method, and BIGPAST. This procedure is repeated one million times. The results, presented in Table 2, indicate that BIGPAST outperforms the other methods in terms of false positive rate (FPR) and accuracy (ACC) when all single-subject observations are from the ground true distribution.

	n	z	t	CG	AD	BIGPAST
FPR	50	0.070022	0.066415	0.066427	0.073271	0.051883
	100	0.069632	0.067787	0.067786	0.056572	0.053742
	200	0.066616	0.065660	0.065668	0.057564	0.052586
	400	0.067888	0.067435	0.067436	0.056244	0.052051
ACC	50	0.929978	0.933585	0.933573	0.926729	0.948117
	100	0.930368	0.932213	0.932214	0.943428	0.946258
	200	0.933384	0.934340	0.934332	0.942436	0.947414
	400	0.932112	0.932565	0.932564	0.943756	0.947949

Table 2: The table presents the simulation results for false positive rate (FPR) and accuracy (ACC), derived from single-subject observations that are exclusively negative, under the assumption that the direction of the alternative hypothesis is ‘less’. Each entry in the table is computed based on one million test outcomes. The abbreviations ‘CG’ and ‘AD’ denote the Crawford-Garthwaite Bayesian and Anderson-Darling methods, respectively.

Given that all single-subject observations are from ground true distribution, implying a negative underlying result, the true positive rate and false negative rate (type II error) are undefined. To address this, we modify the generation of single-subject observations such that 50% yield negative results and the remaining 50% yield positive results. These observations are generated using the method described in Section 3.4. The simulation is then conducted as previously described. The true positive rate and false negative rate for the z score, t score, Crawford-Garthwaite Bayesian method, Anderson-Darling method, and BIGPAST, pertaining to a two-sided test, are presented in Table 3. Similar simulations have been conducted for the alternative hypotheses ‘greater’ and ‘less’, with the results detailed in the Appendix, see Tables 6 and 7.

We can conclude that BIGPAST outperforms the t -score and Crawford-Garthwaite methods in terms of false positive rate (FPR) and accuracy (ACC) when the single-subject observations are mixed. As normal distribution is a special case of skewed Student’s t distribution ($\alpha = 0, \nu = +\infty$), the performance of BIGPAST is still as good as those of t -score and Crawford-Garthwaite methods when the underlying distribution is normal distribution, see Table 8 in Appendix. The results are not surprising because the errors in this context originate from two primary sources: model misspecification and inherent randomness. Notably, BIGPAST is capable of effectively mitigating the errors arising from model misspecification; see Figure 2 in the next section.

	n	z	t	CG	AD	BIGPAST
FPR	50	0.1320	0.1182	0.1182	0.1107	0.0428
	100	0.1269	0.1199	0.1199	0.0782	0.0349
	200	0.1207	0.1166	0.1167	0.0644	0.0334
	400	0.1236	0.1215	0.1215	0.0368	0.0187
TPR	50	0.6908	0.6502	0.6502	0.9101	0.8327
	100	0.6597	0.6415	0.6416	0.9356	0.8992
	200	0.6420	0.6312	0.6311	0.9655	0.9552
	400	0.6316	0.6264	0.6264	0.9660	0.9413
ACC	50	0.7794	0.7660	0.7660	0.8997	0.8949
	100	0.7664	0.7608	0.7609	0.9287	0.9322
	200	0.7606	0.7573	0.7572	0.9505	0.9609
	400	0.7540	0.7525	0.7524	0.9646	0.9613

Table 3: The simulation results of false positive rate (FPR), true positive rate (TPR) and accuracy (ACC), derived from single-subject observations that consist of 50% positive and 50% negative, are presented under the assumption that the alternative hypothesis is ‘two-sided’. Each cell in the resulting table is calculated based on one million test outcomes. ‘CG’ and ‘AD’ represent the Crawford-Garthwaite Bayesian and the Anderson-Darling methods, respectively.

3.3 Model Misspecification Error

In this section, we conduct a comparative analysis of the BIGPAST, CG, and AD methodologies under varying alternative hypotheses and parameter configurations. The predetermined significant level is 0.05. The skewness parameter α and degree of freedom ν are assigned values from the sets (1, 10), (1, 5), (2, 5), and (3, 5), respectively. The location and scale of skewed Student’s t distribution are set to 0 and 1, respectively. Other sample settings include a sample size $n = 100$, $c_\nu = 1$, and a Metropolis-Hastings sampling size of 2000. The comparison procedures are as follows: Firstly, $N = 200$ independent samples are randomly generated from the skewed Student’s t distribution with parameters α and ν . Secondly, $m = 1000$ single-subjects are randomly drawn, and the BIGPAST, CG, and AD tests are conducted on each of the N samples. Thirdly, for each of N samples, the type I error (false positive rate), power (true positive rate), and accuracy are calculated based on the $m = 1000$ single-subjects. Finally, the type I error, power, and accuracy are reported in the form of boxplots for the four skewed Student’s t parameter settings, as shown in Figures 1 and 9 to 11.

Under the mechanism of these parameter settings, the model is misspecified for the CG test. The theoretical assumption of CG test is the normal distribution, the mean and variance can be directly computed from the skewed Student’s t distribution by $\mu = \delta b_\nu, \nu > 1$ and $\sigma^2 = \nu/(\nu - 2) - (b_\nu \delta)^2, \nu > 2$, where

$$b_\nu = \frac{\sqrt{\nu} \Gamma\left(\frac{1}{2}(\nu - 1)\right)}{\sqrt{\pi} \Gamma\left(\frac{\nu}{2}\right)}, \quad \nu > 1; \quad \delta = \frac{\alpha}{\sqrt{1 + \alpha^2}}.$$

We utilise the total variation distance to quantify the disparity between skewed Student’s t (for BIGPAST) and normal (for CG) distributions. The total variation distances of the aforementioned four settings are: 0.057, 0.111, 0.155 and 0.186, respectively, as illustrated in Figures 1a, 9a, 10a and 11a. In the context of a ‘two-sided’ hypothesis test, the divergence between the BIGPAST and CG methodologies becomes larger as the total variation distance increases, as

shown in Figures 1 and 9 to 11. The results of the AD approach demonstrate robustness for different total variation distances, but perform significantly worse than BIGPAST in terms of type I error, as seen in Figure 1b. The AD approach also performs slightly worse than BIGPAST in terms of accuracy, as depicted in Figure 1d.

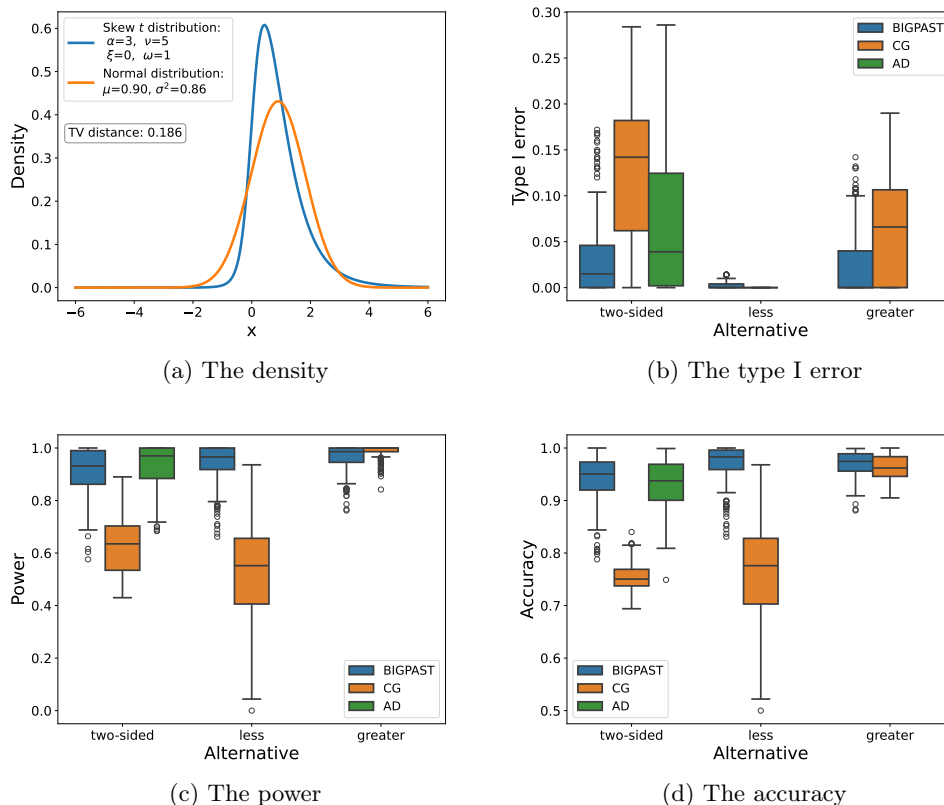


Figure 1: The comparison results of BIGPAST, CG and AD approaches under three alternative hypotheses: ‘two-sided’, ‘less’ and ‘greater’ respectively when $\alpha = 3$ and $\nu = 5$. Figure 1a shows the densities of skewed Student’s t and normal distributions, the μ and σ^2 of normal distribution are equal to the mean and variance of skewed Student’s t distribution. In fact, the normal distribution is the theoretical assumption of the CG test when the sample comes from the skewed Student’s t distribution. AD test is a nonparametric test; there is one result that is compared in the ‘two-sided’ category. TV distance is short for total variation distance. Each boxplot summarises over 200 independent replications.

The complexity of the ‘one-sided’ test compared to the ‘two-sided’ test due to the skewed Student’s t distribution increases due to skewed Student’s t distribution has light and heavy tails. The model misspecification error impacts the tails of the skewed Student’s t distribution differently. When $\alpha > 0$, the heavy tail is on the right side of the mode of the skewed Student’s t distribution. In this paragraph, we explore the scenario where the direction of the alternative hypothesis is ‘greater’. If we implement the CG test, the 95% quantile of normal distribution is less than the 95% quantile of skewed Student’s t distribution. Consequently, the type I error of the CG test exceeds that of the BIGPAST test, leading to a higher power for the CG test,

as shown in Figures 1b and 1c. This can be explained by the light-red region between the 95% quantile of skewed Student’s t distribution and the 95% quantile of normal distribution, as depicted in Figure 2b. Theoretically, all single-case observations from this region will be classified as positive by the CG test and as negative by the BIGPAST test, leading us to refer to this region as the false positive region. The error generated by the false positive region arises from model misspecification rather than sampling randomness, as illustrated in Figure 2.

Conversely, for the light tail of the skewed Student’s t distribution, the 5% quantile of the normal distribution is less than the 5% quantile of the skewed Student’s t distribution. Given that the alternative is ‘less’ and $\alpha > 0$, the region between the 5% quantile of skewed Student’s t distribution and the 5% quantile of the normal distribution is referred to as the false negative region other than the false positive region. Because all the single-case observations from this region will be classified as negative by the CG test, but as positive by the BIGPAST test. Consequently, the theoretical type I error is zero, excluding the random error of sampling, as depicted in Figure 1b. The power of the CG test, i.e., the actual positive rate, is lower than that of the BIGPAST test, as illustrated in Figure 1c.

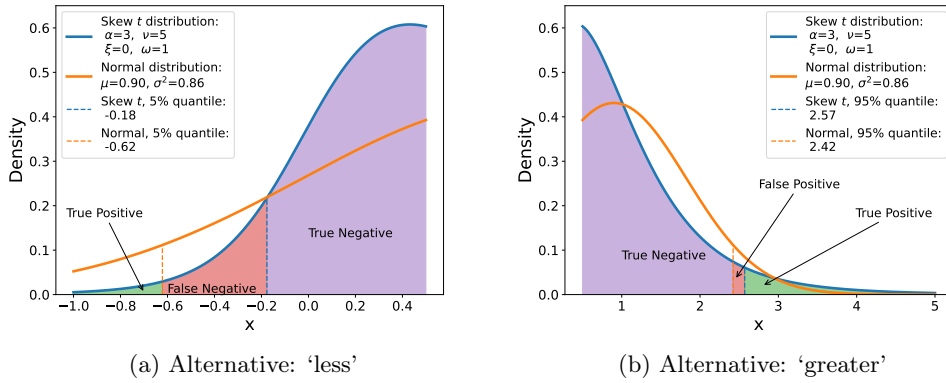


Figure 2: Model misspecification error on the light and heavy tails for one-sided test.

For the left skewed Student’s t distribution ($\alpha < 0$), we can obtain similar results just by reflecting the densities in line $x = 0$. This will not be detailed here. From the preceding discussion, we can conclude that (1) The difference between the BIGPAST and CG methodologies becomes more significant in terms of type I error, power, and accuracy as the total variation distance increases; (2) Assuming a skewed Student’s t distribution, the BIGPAST approach outperforms the CG approach in terms of accuracy due to the presence of model misspecification error; (3) Given the asymmetry between the light and heavy tails of the skewed Student’s t distribution, we recommend using a two-sided test instead of a one-sided test. This is because the combinations of a one-sided test (‘less’ or ‘greater’) and the sign of α significantly influence the evaluation of detection.

3.4 Comparison Study with Other Frameworks

This section is dedicated to assessing the performance of the proposed BIGPAST methodology and existing approaches when a control group is present. The first approach is a variant of BIGPAST based on the maximum a posteriori (MAP) estimation. Specifically, procedures 3-5 of the BIGPAST are simplified into the following two steps:

- 3' Obtain the maximum posterior estimators of α, ν, ξ, ω by maximising the posterior distribution $\boldsymbol{\pi}(\alpha, \nu, \xi, \omega | \mathbf{x})$, denoted as $\hat{\alpha}_{\text{MAP}}, \hat{\nu}_{\text{MAP}}, \hat{\xi}_{\text{MAP}}, \hat{\omega}_{\text{MAP}}$.
- 4' Given the significance level α^* , the credible interval of x^* given \mathbf{x} is $[x_{\alpha^*/2}^{\text{MAP}}, x_{1-\alpha^*/2}^{\text{MAP}}]$, where $x_{\alpha^*/2}^{\text{MAP}}$ and $x_{1-\alpha^*/2}^{\text{MAP}}$ are the $\alpha^*/2$ and $1 - \alpha^*/2$ quantiles of $\boldsymbol{\pi}(\hat{\alpha}_{\text{MAP}}, \hat{\nu}_{\text{MAP}}, \hat{\xi}_{\text{MAP}}, \hat{\omega}_{\text{MAP}} | \mathbf{x})$, respectively. If x^* does not fall within this credible interval, then the null hypothesis \mathcal{H}_0 can be rejected at the significance level α^* .

The second approach is a non-Bayesian approach that relies on maximum likelihood estimation (MLE). This approach operates under the sole assumption that the control group follows a skewed Student's t distribution. The MLE procedures can be outlined as follows:

- 1' Obtain the maximum likelihood estimators of α, ν, ξ, ω by maximising the likelihood function $l(\mathbf{x} | \alpha, \nu, \xi, \omega)$. These estimators are denoted as $\hat{\alpha}_{\text{MLE}}, \hat{\nu}_{\text{MLE}}, \hat{\xi}_{\text{MLE}}, \hat{\omega}_{\text{MLE}}$.
- 2' Given the significance level α^* , the confidence interval of x^* given \mathbf{x} is $[x_{\alpha^*/2}^{\text{MLE}}, x_{1-\alpha^*/2}^{\text{MLE}}]$, where $x_{\alpha^*/2}^{\text{MLE}}$ and $x_{1-\alpha^*/2}^{\text{MLE}}$ are the $\alpha^*/2$ and $1 - \alpha^*/2$ quantiles of $f_c(\hat{\alpha}_{\text{MLE}}, \hat{\nu}_{\text{MLE}}, \hat{\xi}_{\text{MLE}}, \hat{\omega}_{\text{MLE}})$, respectively. If x^* does not fall within this confidence interval, then the null hypothesis \mathcal{H}_0 can be rejected at the significance level α^* .

The third approach is a non-parametric (NP) approach. Given group data \mathbf{x} and a significant level α^* , we can derive the empirical confidence interval $[x_{(\lfloor n^* \alpha^*/2 \rfloor)}^{\text{NP}}, x_{(\lceil n^* (1-\alpha^*/2) \rceil)}^{\text{NP}}]$ where $x_{(\lfloor n^* \alpha^*/2 \rfloor)}^{\text{NP}}$ and $x_{(\lceil n^* (1-\alpha^*/2) \rceil)}^{\text{NP}}$ are the empirical quantiles of \mathbf{x} at $\alpha^*/2$ and $1 - \alpha^*/2$, respectively. If x^* does not fall within this empirical confidence interval, then the null hypothesis \mathcal{H}_0 can be rejected at the significance level α^* . The NP approach does not rely on any distributional assumptions. Given that our BIGPAST methodology employs the Metropolis-Hastings sampler in Step 3, we will refer to the aforementioned four approaches: MH, MAP, MLE, and NP, respectively.

We now outline the data generation mechanism for a single-subject and control group. Given the parameters α, ν, ξ, ω , we randomly draw N independent control groups $\mathbf{x}_1, \mathbf{x}_2, \dots, \mathbf{x}_N$ from $f_c(\alpha, \nu, \xi, \omega)$. The following is a straightforward method for generating single-subject data. Define $S_1 := (-\infty, q_{2.5\%}] \cup [q_{97.5\%}, \infty)$ and $S_2 := (q_{2.5\%}, q_{5\%}] \cup [q_{95\%}, q_{97.5\%})$ where $q_{2.5\%}, q_{5\%}, q_{95\%}, q_{97.5\%}$ are 0.025, 0.05, 0.95, 0.975 quantiles of $f_c(\alpha, \nu, \xi, \omega)$. We draw k_1 and k_2 random copies of single-subjects $x_1^* \dots, x_{k_1}^*, x_{k_1+1}^*, \dots, x_{k_1+k_2}^*$ respectively from the uniform distributions defined on S_1 and S_2 . Let $K = k_1 + k_2$. At the significant level of 0.05, the ground truth for the first k_1 single-subjects is negative, while the ground truth for the remaining k_2 single-subjects is positive. In the simulation, we first apply the MH, MAP, MLE, and NP approaches to $\mathbf{x}_i, i = 1, 2, \dots, N$ to obtain the four types of intervals. Next, we conduct the hypothesis tests by comparing $\mathbf{x}^* = (x_1^*, x_2^*, \dots, x_K^*)$ with each type of intervals. Finally, we compute the false discovery rate (FDR) and accuracy (ACC) defined by

$$\text{FDR}_i^{\mathcal{M}} := \frac{\text{FP}_i^{\mathcal{M}}}{\text{TP}_i^{\mathcal{M}} + \text{FP}_i^{\mathcal{M}}}, \quad \text{ACC}_i^{\mathcal{M}} := \frac{\text{TP}_i^{\mathcal{M}} + \text{TN}_i^{\mathcal{M}}}{K}, \quad i = 1, 2, \dots, N,$$

where TP, FP, and TN represent the number of true positive, false positive and true negative, respectively. \mathcal{M} could be one of MH, MAP, MLE, NP.

The parameters settings are as follows: we consider ten combinations of (α, ν) : (0,3), (1,3), (3,3), (5,5), (10,10), (20,20), (30,30), (50,50), (5,50) and (50,5) with fixed $\xi = -2$ and $\omega = 2$. In MH approach, we let $m = 5000, s = 100$ and $c_\nu = 1$. The other parameter settings are $N = 400, n = 100, k_1 = k_2 = 1000, \alpha^* = 0.05$. The results are presented in [Table 4](#) and [Figure 3](#).

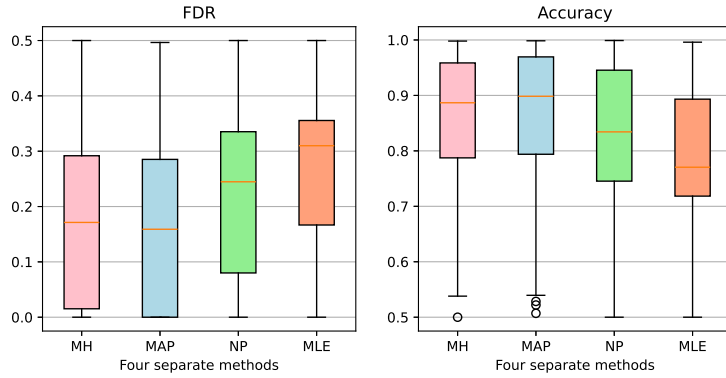
Table 4 displays the FDR and ACC of the four approaches. The MH and MAP approaches consistently outperform the NP and MLE approaches in terms of FDR and ACC. When $|\alpha| \leq 3$ and $\nu \leq 3$, both the FDR and ACC of the MAP approach surpass those of the MH approach. This is expected, as the MAP approach provides more accurate estimation of the underlying parameters of the skewed Student’s t distribution when $|\alpha|$ and ν are small, as is shown in column 3 of Table 1. When $|\alpha|$ or ν is large, the FDR and ACC of the MH approach perform better than those of the MAP approach. This can be attributed to the randomness of parameters in the Metropolis-Hastings sampler. However, the MAP approach fails to estimate the underlying parameters when α or ν is large, as is shown in column 4 of Table 1, and lacks randomness of parameters. The boxplots in Figure 3 clearly illustrate the comparison between the MH and MAP approaches. The results illustrate that the FDR of MH (i.e. BIGPAST) is generally lower than others, and the ACC of MH (i.e. BIGPAST) is generally greater than other methods in conducting hypothesis tests for single-subject data.

(α, ν)	FDR				ACC			
	MH	MAP	NP	MLE	MH	MAP	NP	MLE
(0,3)	0.174	0.165	0.216	0.266	0.865	0.872	0.833	0.787
(1,3)	0.158	0.145	0.201	0.257	0.877	0.888	0.845	0.797
(3,3)	0.142	0.129	0.197	0.254	0.891	0.901	0.849	0.798
(5,5)	0.131	0.136	0.206	0.255	0.905	0.899	0.846	0.803
(10,10)	0.118	0.145	0.200	0.259	0.915	0.894	0.851	0.797
(20,20)	0.132	0.157	0.190	0.255	0.907	0.886	0.861	0.803
(30,30)	0.132	0.171	0.188	0.261	0.907	0.875	0.862	0.796
(50,50)	0.134	0.184	0.193	0.254	0.906	0.864	0.859	0.801
(5,50)	0.144	0.158	0.185	0.261	0.898	0.885	0.865	0.796
(50,5)	0.139	0.165	0.218	0.249	0.899	0.876	0.834	0.805

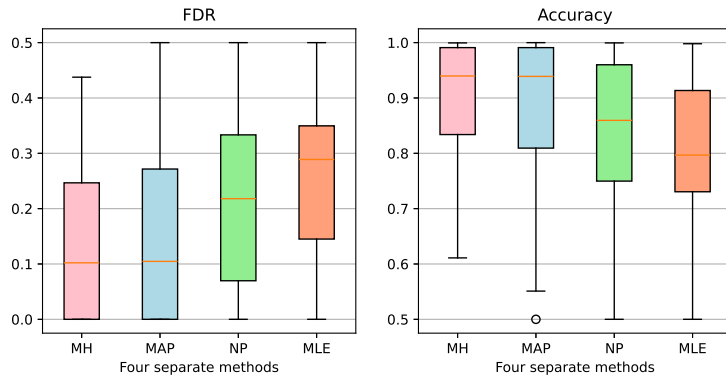
Table 4: The average false discovery rate (FDR) and accuracy (ACC) for the MH, MAP, MLE, and NP approaches, calculated over 400 repetitions. In this context, MH refers to the original BIGPAST method, MAP denotes the Bayesian inference framework based on maximum a posteriori estimation, MLE represents the method based on maximum likelihood estimation, and NP signifies the non-parametric method.

4 Real Data Analysis

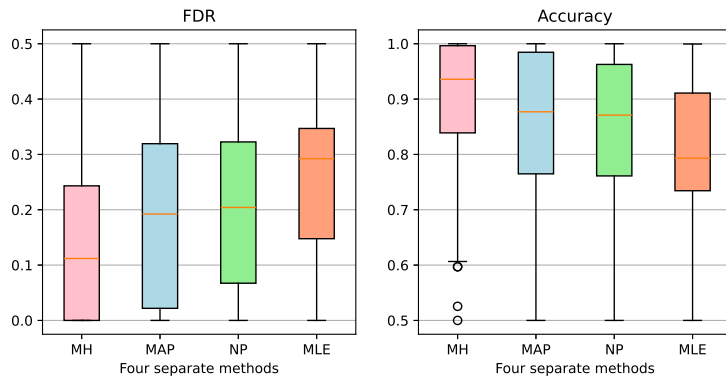
This dataset is derived from a mild traumatic brain injury (mTBI) study conducted by [Innovision IP Ltd.](#) It comprises functional time series of Magnetoencephalography (MEG) data and an anatomical T1-weighted Magnetic Resonance Imaging (MRI) scan for 103 healthy subjects and one patient with mild traumatic brain injury. The MEG data, recorded from 306 sensors, was pre-processed using the ‘MNE-Python’ package ([Gramfort et al., 2013](#)). The MEG data was analysed to reconstruct the source generators using a minimum norm inverse method. The MRI data was pre-processed with the ‘FreeSurfer’ package ([Han et al., 2006](#)). The standard FreeSurfer pipeline (detailed on their website) was followed and includes motion correction, intensity normalisation, skull-stripping, normalisation to template space and segmentation of the cortex and subcortical structures using the Desikan-Killiany atlas. This results in 68 regions covering the entire cortex. For each cortical region, we calculate the average of source powers within this region. This process yields a control group dataset with dimensions $103 \times 68 \times 100$ and a patient dataset



(a) $\alpha = 0, \nu = 3$



(b) $\alpha = 5, \nu = 5$



(c) $\alpha = 50, \nu = 50$

Figure 3: The boxplots for false discovery rate (FDR) and accuracy (ACC) of the MH, MAP, MLE, and NP approaches for three distinct skewness parameters: low ($\alpha = 0$), medium ($\alpha = 5$), and high ($\alpha = 50$). In this context, MH refers to the original BIGPAST method, MAP denotes the Bayesian inference framework based on maximum a posteriori estimation, MLE represents the method based on maximum likelihood estimation, and NP signifies the non-parametric method.

with dimensions 68×100 . To simplify, we treat the epochs as repeated observations and take average over them to reduce the data’s complexity. Consequently, the control group dataset has dimensions 103×68 , and the patient dataset is reduced to a vector of length 68.

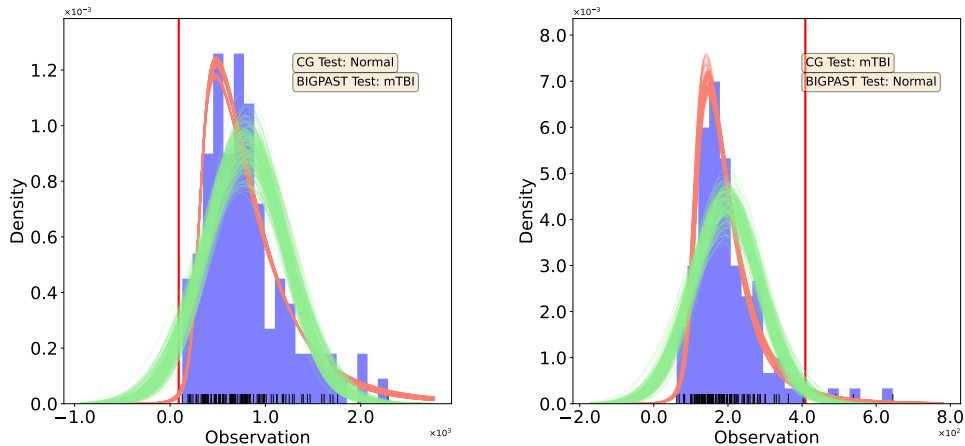
For each brain region of the Desikan-Killiany cortical atlas, we apply the BIGPAST method to the control group and patient dataset to test whether the patient significantly differs from the control group. In this real data analysis, we know that the single-subject has mTBI. However, in practice, we can calculate the observation of a new client and conduct the hypothesis test using BIGPAST to determine whether the client significantly differs from the control group.

We further explore the impact of waveband frequency on the comparison between a control group and a single-subject. The wavebands are arranged in ascending order of frequency: delta (1-4 Hz), theta (4-8 Hz), alpha (8-12 Hz), beta (12-30 Hz), and gamma (30-45 Hz). The subsequent results also include their findings, denoted as CG for brevity. The prespecified significant level is 0.05.

(CG, BIGPAST)	delta	theta	alpha	beta	gamma
(mTBI, mTBI)	6,17, 40,51	4,6, 17,48	6,14, 17,40	6,12,17, 38,40	17
(Normal, mTBI)	1,10,16,26, 35,50,59,62	1,2,24, 35,62	2,24,35, 58,59	1,2,10,22, 24,35,59	1,2,35
(mTBI, Normal)	NA	14,40	NA	14,47	6,40
(Normal, Normal)	Others	Others	Others	Others	Others

Table 5: The test results of the Crawford-Garthwaite (CG) and BIGPAST approaches, both based on the normal and skewed Student’s t assumptions. The indices corresponding to specific brain cortical regions are 1: lh-caudal anterior cingulate, 2: lh-caudal middle frontal, 4: lh-entorhinal, 6: lh-fusiform, 10: lh-isthums cingulate, 12: lh-lateral orbitofrontal, 14: lh-medial orbitofrontal, 17: lh-parahippocampal, 22: lh-postcentral, 24: lh-precentral, 26: lh-rostral anterior cingulate, 35: rh-caudal anterior cingulate, 38: rh-entorhinal, 40: rh-fusiform, 47: rh-lingual, 50: rh-paracentral, 51: rh-parahippocampal, 58: rh-precentral, 59: rh-precuneus, 62: rh-superior frontal. The prefixes ‘lh-’ and ‘rh-’ indicate the left and right hemispheres of the brain, respectively. ‘NA’ stands for ‘not available’, and ‘Others’ represents the remaining brain cortical indices not listed in the column, but can be found the indices in [Table 9](#).

In this real data analysis, the null hypothesis is two-sided, with one heavy tail and one light tail in the skewed Student’s t distribution. The cortical region indices in row 3 of [Table 5](#) exhibit a positive skewness parameter, i.e., $\alpha > 0$. Consequently, the light tail is on the left, and the heavy tail is on the right. For all cortical region indices in row 3 of [Table 5](#), the single-subject observation is located at the light tail of the skewed Student’s t distribution. This positioning suggests a high probability of rejecting the null hypothesis based on the skewed Student’s t assumption, as illustrated in [Figure 4a](#). Similarly, for cortical regions 6 (lh-fusion, gamma band), 14 (lh-medial orbitofrontal, theta and beta bands), 40 (rh-fusiform, theta and gamma bands), and 47 (rh-lingual, beta band), the single-subject observation is located at the heavy tail of the skewed Student’s t distribution, as shown in [Figure 4b](#). The skewed Student’s t assumption is more appropriate for these cortical regions than the assumption of normal distribution. The BIGPAST approach outperforms the CG approach in detecting the single-subject observation at the heavy tail of the skewed Student’s t distribution, as demonstrated in [Figure 4](#). Because the BIGPAST approach corrects the model misspecification error at both tails compared to the CG



(a) Delta Band, $\bar{\alpha} \approx 3.95$, Left Caudal Anterior Cingulate (b) Gamma Band, $\bar{\alpha} \approx 2.69$, Right Fusiform Cingulate

Figure 4: The comparison results between the Crawford-Garthwaite (CG) and BIGPAST approaches in terms of density estimations. The light-red lines represent the skewed Student’s t densities, with parameters drawn from the BIGPAST approach’s posterior distribution. The light green lines depict the normal densities, with parameters drawn from the CG approach’s posterior distribution. The CG test is based on 10,000 densities, while the BIGPAST test is based on 5,000 densities (the first 5,000 densities are discarded for burn-in). For clarity, each panel only displays 200 densities drawn from the CG and BIGPAST posterior distribution. The red vertical line on the x axis represents the observation of a single-subject (i.e., a patient with mTBI). A histogram is used to demonstrate the goodness of fit for both the CG and BIGPAST approaches.

approach. By combining rows 2 and 3 of Table 5 and Figure 4, we conclude that the BIGPAST approach is more reliable than the CG approach in hypothesis tests for single-subject data when the control group data exhibits skewness.

5 Conclusion

In this paper, we proposed a novel Bayesian inference framework for the abnormality detection on a single-subject versus a control group. Under the assumption of a normal distribution, the t -score (Crawford and Howell, 1998) is capable of managing scenarios where the sample size is fewer than 30 (Machin et al., 2018). However, in neuroscience, the number of epochs often exceeds 100, sometimes even reaching 1000, and the distributions—whether over epochs or subjects—exhibit skewness. Under these conditions, methods predicated on the assumption of normality cease to be effective. Our proposed methodology, BIGPAST, leverages the skewed Student’s t distribution, effectively capturing the inherent asymmetry of the data.

In terms of accuracy, power, and type I error, our proposed BIGPAST methodology surpasses the existing Crawford-Garthwaite (CG) approach. Particularly when the control group data exhibits skewness, BIGPAST provides a more reliable solution for hypothesis testing on single-subject data. Furthermore, BIGPAST demonstrates superior robustness to model mis-

specification errors compared to the CG approach. The performance of the BIGPAST and CG methodologies is significantly influenced by the total variation distance between the skewed Student's t distribution and the normal distribution. When this distance is large, the BIGPAST approach exhibits superior accuracy compared to the CG method. The skewed Student's t distribution's asymmetry, characterised by its light and heavy tails, further emphasises the necessity of employing a two-sided test over a one-sided test.

The BIGPAST framework can be readily adapted to accommodate other distributions, such as Sub-normal, Sub-Weibull, or Extreme Value distributions. The key requirement is to identify an appropriate prior distribution for the parameters of the chosen distribution. A further extension of BIGPAST could encompass multivariate distributions, thereby enabling the application of the BIGPAST methodology to high-dimensional data in future.

References

- Azzalini, A. and A. Capitanio (2003). Distributions generated by perturbation of symmetry with emphasis on a multivariate skew t -distribution. *Journal of the Royal Statistical Society: Series B (Statistical Methodology)* 65(2), 367–389.
- Azzalini, A. and A. Capitanio (2014, January). *The skew-normal and related families*. Number 3 in Institute of Mathematical Statistics monographs. Cambridge: Cambridge University Press.
- Bayes, C. L. and M. D. Branco (2007). Bayesian inference for the skewness parameter of the scalar skew-normal distribution. *Brazilian Journal of Probability and Statistics* 21(2), 141–163.
- Branco, M. D., M. G. Genton, and B. Liseo (2013). Objective Bayesian analysis of skew- t distributions. *Scandinavian Journal of Statistics* 40(1), 63–85.
- Buzsáki, G. and K. Mizuseki (2014, April). The log-dynamic brain: how skewed distributions affect network operations. *Nature Reviews Neuroscience* 15(4), 264–278.
- Chen, G. and N. Balakrishnan (1995). A general purpose approximate goodness-of-fit test. *Journal of Quality Technology* 27(2), 154–161.
- Crawford, J. R. and P. H. Garthwaite (2006, September). Methods of testing for a deficit in single-case studies: Evaluation of statistical power by monte carlo simulation. *Cognitive Neuropsychology* 23(6), 877–904.
- Crawford, J. R. and P. H. Garthwaite (2007). Comparison of a single case to a control or normative sample in neuropsychology: development of a bayesian approach. *Cognitive Neuropsychology* 24(4), 343–372.
- Crawford, J. R., P. H. Garthwaite, A. Azzalini, D. C. Howell, and K. R. Laws (2006, January). Testing for a deficit in single-case studies: Effects of departures from normality. *Neuropsychologia* 44(4), 666–677.
- Crawford, J. R. and D. C. Howell (1998, November). Comparing an individual's test score against norms derived from small samples. *The Clinical Neuropsychologist* 12(4), 482–486.
- Dette, H., C. Ley, and F. Rubio (2018). Natural (non-)informative Priors for skew-symmetric distributions. *Scandinavian Journal of Statistics* 45(2), 405–420.
- Fonseca, T. C. O., M. A. R. Ferreira, and H. S. Migon (2008). Objective bayesian analysis for the student- t regression model. *Biometrika* 95(2), 325–333.
- Gramfort, A., M. Luessi, E. Larson, D. A. Engemann, D. Strohmeier, C. Brodbeck, R. Goj, M. Jas, T. Brooks, L. Parkkonen, and M. S. Hämäläinen (2013). MEG and EEG data analysis with MNE-python. *Frontiers in Neuroscience* 7(267), 1–13.

- Han, X., J. Jovicich, D. Salat, A. van der Kouwe, B. Quinn, S. Czanner, E. Busa, J. Pacheco, M. Albert, R. Killiany, P. Maguire, D. Rosas, N. Makris, A. Dale, B. Dickerson, and B. Fischl (2006). Reliability of mri-derived measurements of human cerebral cortical thickness: the effects of field strength, scanner upgrade and manufacturer. *NeuroImage* 32(1), 180–194.
- Hastings, W. K. (1970). Monte carlo sampling methods using markov chains and their applications. *Biometrika* 57(1), 97–109.
- Ismail, S., W. Sun, F. S. Nathoo, A. Babul, A. Moiseev, M. F. Beg, and N. Virji-Babul (2013, August). A skew-t space-varying regression model for the spectral analysis of resting state brain activity. *Statistical Methods in Medical Research* 22(4), 424–438.
- Jeffreys, H. (1946). An invariant form for the prior probability in estimation problems. *Proceedings of the Royal Society of London. Series A, Mathematical and Physical Sciences* 186(1007), 453–461.
- Machin, D., M. J. Campbell, S. B. Tan, and S. H. Tan (2018). *Sample sizes for clinical, laboratory and epidemiology studies*. John Wiley & Sons.
- Rubio, F. J. and M. F. J. Steel (2014). Inference in two-piece location-scale models with Jeffreys priors. *Bayesian Analysis* 9(1), 1–22.
- Scholz, F. W. and M. A. Stephens (1987). K-sample anderson-darling tests. *Journal of the American Statistical Association* 82(399), 918–924.
- Sun, D. and J. O. Berger (1998). Reference priors with partial information. *Biometrika* 85(1), 55–71.
- Taylor, C. A., J. M. Bell, M. J. Breiding, and L. Xu (2017, MAR 17). Traumatic brain injury-related emergency department visits, hospitalizations, and deaths - united states, 2007 and 2013. *MMWR SURVEILLANCE SUMMARIES* 66(9), 1–18.

A Appendix

Lemma A.1. Let $t(z|\nu)$ and $T(z|\nu)$ be the probability density function and cumulative distribution function of the Student's t -distribution, respectively, for $\nu \geq 1$, then $t(z|\nu)[T(z|\nu)]^{-1/2}[1 - T(z|\nu)]^{-1/2}/\pi$ can be approximated by $t(z/\sigma_\nu|\nu)/\sigma_\nu$, where $\sigma_\nu = 1.5536$ if $\nu > 2400$. If $1 \leq \nu \leq 2400$, then

$$\begin{aligned} \sigma_\nu = & 0.00000543(\log(\nu))^7 - 0.00016303(\log(\nu))^6 + 0.00199613(\log(\nu))^5 - 0.01285016(\log(\nu))^4 \\ & + 0.04631303(\log(\nu))^3 - 0.08761023(\log(\nu))^2 + 0.05036188 \log(\nu) + 1.62021189 \end{aligned} \quad (3)$$

Proof. Firstly, when $1 \leq \nu \leq 2400$, we can use $t(z/\sigma_\nu|\nu)/\sigma_\nu$ to approximate $t(z|\nu)[T(z|\nu)]^{-1/2}[1 - T(z|\nu)]^{-1/2}/\pi$ by the similar discussion in [Bayes and Branco \(2007\)](#). Apparently, the optimal scale σ_ν depends on ν . To obtain [Equation \(3\)](#), for simplicity, let $f := t(z|\nu)[T(z|\nu)]^{-1/2}[1 - T(z|\nu)]^{-1/2}/\pi$ and $g := t(z/\sigma_\nu|\nu)/\sigma_\nu$. Define the total variational distance between f and g as

$$TV(\sigma_\nu) := TV(f, g) = \frac{1}{2} \int_{-\infty}^{\infty} |f - g| dz \quad (4)$$

Let

$$\nu_i = \begin{cases} 0.5 + 0.5i & i = 1, 2, \dots, 199 \\ 100 + 50 * (i - 199) & i = 200, 201, \dots, 245, \end{cases}$$

given ν_i , we use grid search method to minimise $KL(\sigma(\nu_i))$ and obtain the optimal scale $\hat{\sigma}(\nu_i)$. Let $\sigma_{j, \nu_i} = 1 + 0.0002j$, $j = 0, 1, \dots, 5000$, then $\hat{\sigma}_{\nu_i} = \arg \min_{\sigma_{j, \nu_i}} KL(\sigma_{j, \nu_i})$ where $KL(\sigma_{j, \nu_i})$ is evaluated using the Monte Carlo method. Finally, we carry out the polynomial fit with polynomial degree $p = 2, 3, \dots, 7$ based on the optimal scale $\hat{\sigma}(\nu_i)$ and $\log(\nu_i)$, $i = 1, 2, \dots, 245$. [Equation \(3\)](#) is the best polynomial fit with polynomial degree $p = 7$ based on Bayes information criterion, see [Figure 5](#). Secondly, when $\nu > 2400$, $t(z|\nu)[T(z|\nu)]^{-1/2}[1 - T(z|\nu)]^{-1/2}/\pi$ can be approximated by $\phi(z)[\Phi(z)]^{-1/2}[1 - \Phi(z)]^{-1/2}/\pi$. According to [Bayes and Branco \(2007\)](#), $\phi(z)[\Phi(z)]^{-1/2}[1 - \Phi(z)]^{-1/2}/\pi$ can be further approximated by $N(0, \sigma_\nu^2)$ where the optimal scale σ_ν chosen by total variational distance is 1.5536. Note that [Bayes and Branco \(2007\)](#) used the optimal scale σ_ν chosen by the Kullback-Leibler divergence (defined in [Equation \(5\)](#)), the optimal scale σ_ν is 1.54 for normal distribution. However, our simulation result shows that the total variational distance criterion performs better than the Kullback-Leibler divergence criterion for Student's t with a small degree of freedom, see [Figure 6](#). Therefore, we employ the criterion of total variational distance to choose the optimal scale σ_ν in $t(z/\sigma_\nu|\nu)/\sigma_\nu$ to approximate $t(z|\nu)[T(z|\nu)]^{-1/2}[1 - T(z|\nu)]^{-1/2}/\pi$ throughout this paper. [Figure 7](#) shows the density $t(z|\nu)[T(z|\nu)]^{-1/2}[1 - T(z|\nu)]^{-1/2}/\pi$ and its approximation $t(z/\sigma_\nu|\nu)/\sigma_\nu$ with σ_ν in [Equation \(3\)](#) for $\nu = 1, 5, 10, 100$.

$$KL(\sigma_\nu) := KL(f, g) = \int_{-\infty}^{\infty} f \log \left(\frac{f}{g} \right) dz + \int_{-\infty}^{\infty} g \log \left(\frac{g}{f} \right) dz. \quad (5)$$

□

Lemma A.2. Let $f(z|\alpha, \nu)$ be the non-linear skewed Student's t density function, defined as follows:

$$f(z|\alpha, \nu) := 2t(z|\nu)T(\alpha z r(z, \nu)|\nu + 1), \quad z \in \mathbb{R}, \alpha \in \mathbb{R}, \nu > 0,$$

where $r(z, \nu) = \sqrt{(\nu + 1)/(v + z^2)}$. Given any $\nu > 0$, let $\pi(\alpha|\nu)$ represent the Jeffery's prior for α , we have

$$\pi(\alpha|\nu) \propto \frac{\sqrt{\pi} \Gamma\left(\frac{\nu}{2} + 1\right) \sqrt{{}_2F_1\left(\frac{1}{2}, \nu + 1; \frac{\nu+1}{2}; -\frac{\alpha^2}{\sigma_{\nu+1}^2}\right) - {}_2F_1\left(\frac{1}{2}, \nu + 2; \frac{\nu+1}{2}; -\frac{\alpha^2}{\sigma_{\nu+1}^2}\right)}}{|\alpha| \Gamma\left(\frac{\nu+1}{2}\right)} \quad (6)$$

, where ${}_2F_1(a, b; c; d)$ represents the hypergeometric function, $\sigma_{\nu+1}$ is defined in [Lemma A.1](#), $\Gamma(\cdot)$ is the Gamma function.

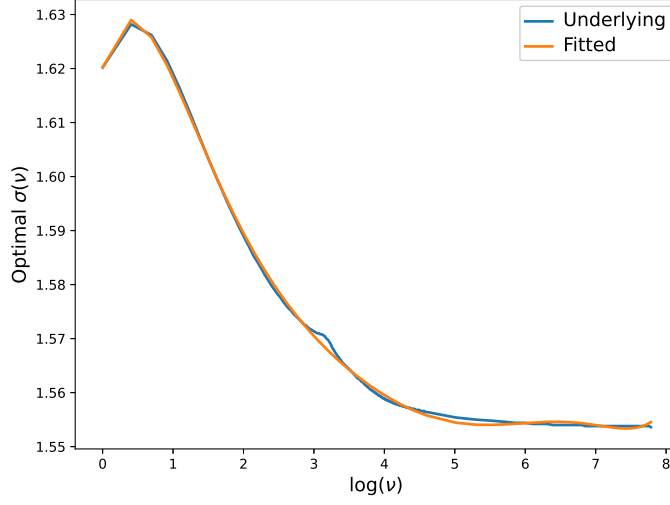


Figure 5: Polynomial fitted curve

Proof. By definition of Jeffery's prior, we have $\pi(\alpha|\nu) \propto \sqrt{I_{\alpha\alpha}}$, where $I_{\alpha\alpha}$ is the Fisher information of α in the non-linear skewed Student's t density function $f(z|\alpha, \nu)$. According to Branco et al. (2013, Proposition 2), the Fisher information of α in $f(z|\alpha, \nu)$ is given by

$$I_{\alpha\alpha} = 2 \int_0^{+\infty} \frac{z^2 r(z, \nu)^2 t(z|\nu) t^2(\alpha z r(z, \nu)|\nu + 1)}{T(\alpha z r(z, \nu)|\nu + 1) [1 - T(\alpha z r(z, \nu)|\nu + 1)]} dz. \quad (7)$$

Let $m = \alpha z r(z, \nu)$, by the change of variable $z = \frac{\sqrt{m^2 \nu}}{\sqrt{\alpha^2 \nu + \alpha^2 - m^2}}$, Equation (7) can be rewritten as

$$I_{\alpha\alpha} = 2 \int_0^{\alpha \sqrt{\nu+1}} \frac{m^2 t\left(\frac{\sqrt{m^2 \nu}}{\sqrt{\alpha^2 \nu + \alpha^2 - m^2}} \middle| \nu\right) t^2(m|\nu + 1)}{T(m|\nu + 1) [1 - T(m|\nu + 1)]} \frac{\sqrt{\nu}(\nu + 1)}{(\alpha^2(\nu + 1) - m^2)^{3/2}} dm. \quad (8)$$

By Lemma A.1, we have $t(m|\nu + 1)[T(m|\nu + 1)]^{-1/2}[1 - T(m|\nu + 1)]^{-1/2}/\pi \approx t(m/\sigma_{\nu+1}|\nu + 1)/\sigma_{\nu+1}$. Substituting this approximation into Equation (8), we obtain

$$I_{\alpha\alpha} \approx 2 \int_0^{\alpha \sqrt{\nu+1}} \frac{m^2 \pi^2 \left(\frac{1}{\frac{m^2}{\alpha^2 \nu + \alpha^2 - m^2} + 1}\right)^{\frac{\nu+1}{2}} \left(\frac{\nu+1}{\frac{m^2}{\sigma_{\nu+1}^2} + \nu+1}\right)^{\nu+2}}{(\alpha^2(\nu + 1) - m^2)^{3/2} \sigma_{\nu+1}^2 B\left(\frac{\nu}{2}, \frac{1}{2}\right) B\left(\frac{\nu+1}{2}, \frac{1}{2}\right)^2} dm, \quad (9)$$

where $B(\cdot, \cdot)$ is the Beta function. Furthermore, let $x = m^2$, by change of variable, Equation (9) can be rewritten as

$$I_{\alpha\alpha} \approx 2 \int_0^{\alpha^2(\nu+1)} \frac{\pi^2 \sqrt{x} \left(\frac{1}{\frac{x}{\alpha^2(\nu+1)} - x} + 1\right)^{\frac{\nu+1}{2}} \left(\frac{\nu+1}{\nu + \frac{x}{\sigma_{\nu+1}^2} + 1}\right)^{\nu+2}}{\sigma_{\nu+1}^2 B\left(\frac{\nu}{2}, \frac{1}{2}\right) B\left(\frac{\nu+1}{2}, \frac{1}{2}\right)^2 (\alpha^2(\nu + 1) - x)^{3/2}} dx. \quad (10)$$

By integration, we obtain the following expression:

$$I_{\alpha\alpha} \approx \frac{\pi \Gamma\left(\frac{\nu}{2} + 1\right)^2 \left({}_2F_1\left(\frac{1}{2}, \nu + 1; \frac{\nu+1}{2}; -\frac{\alpha^2}{\sigma_{\nu+1}^2}\right) - {}_2F_1\left(\frac{1}{2}, \nu + 2; \frac{\nu+1}{2}; -\frac{\alpha^2}{\sigma_{\nu+1}^2}\right) \right)}{\alpha^2 \Gamma\left(\frac{\nu+1}{2}\right)^2},$$

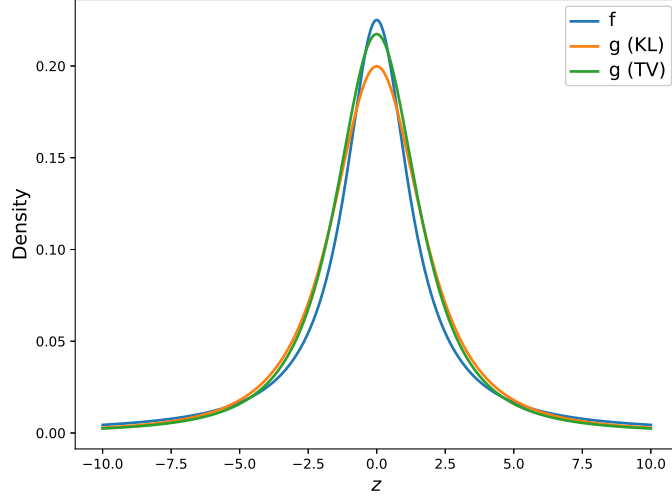


Figure 6: Comparison of approximation based on Kullback-Leibler divergence and total variational distance when the degree of freedom $\nu = 2$. The blue line represents the density of f , the green line represents the density of approximation g based on total variational distance, the orange line is the density of approximation g based on Kullback-Leibler divergence.

which completes the proof. \square

The Proof of Theorem 2.1

Proof. The log-likelihood function of $f(z|\alpha, \nu)$, say $\ell(\alpha, \nu)$, can be expressed as

$$\ell(\alpha, \nu) = \log\left(\frac{2}{\sqrt{\pi}}\right) + \frac{\nu+1}{2} \log\left(\frac{\nu}{\nu+z^2}\right) - \frac{1}{2} \log(\nu) + \log\left(\Gamma\left(\frac{\nu+1}{2}\right)\right) - \log\left(\Gamma\left(\frac{\nu}{2}\right)\right) + \log(T(w|\nu+1)). \quad (11)$$

The derivative of $\ell(\alpha, \nu)$ with respect to ν is given by

$$\frac{\partial \ell(\alpha, \nu)}{\partial \nu} = \frac{1}{2} \log\left(\frac{\nu}{\nu+z^2}\right) - \frac{1}{2} \psi\left(\frac{\nu}{2}\right) + \frac{1}{2} \psi\left(\frac{\nu+1}{2}\right) + \frac{z^2-1}{2(\nu+z^2)} + \frac{1}{T(w|\nu+1)} \frac{\partial T(w|\nu+1)}{\partial \nu}, \quad (12)$$

where $\psi(x) := d \log \Gamma(x) / dx$ is the digamma function. The derivative of $T(w|\nu+1)$ with respect to the

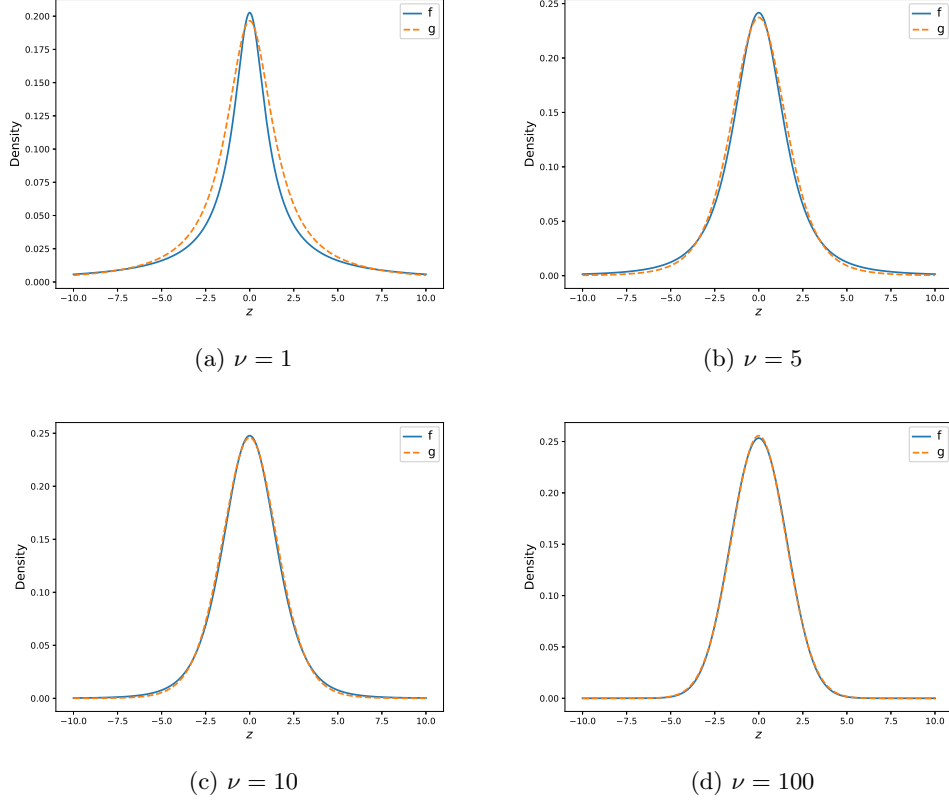


Figure 7: Density f (solid blue curve) and its approximation g with σ_ν (dashed orange curve) for $\nu = 1, 5, 10, 100$.

parameter ν can be expressed by

$$\begin{aligned}
\frac{\partial T(w|\nu+1)}{\partial \nu} &= t(w|\nu+1) \frac{\partial w}{\partial \nu} + \int_{-\infty}^w \frac{\partial t(x|\nu+1)}{\partial \nu} dx \\
&= t(w|\nu+1) \frac{\alpha z (z^2 - 1)}{2\sqrt{\nu+1} (\nu + z^2)^{3/2}} + \frac{1}{2} \left[-\psi \left(\frac{\nu+1}{2} \right) + \psi \left(\frac{\nu}{2} + 1 \right) \right] T(w|\nu+1) \\
&\quad + \int_{-\infty}^w \frac{1}{2} \left[\log \left(\frac{\nu+1}{\nu+x^2+1} \right) + \frac{x^2-1}{(\nu+x^2+1)} \right] t(x|\nu+1) dx \\
&= t(w|\nu+1) \frac{\alpha z (z^2 - 1)}{2\sqrt{\nu+1} (\nu + z^2)^{3/2}} + \frac{1}{2} \left[-\psi \left(\frac{\nu+1}{2} \right) + \psi \left(\frac{\nu}{2} + 1 \right) \right] T(w|\nu+1) \\
&\quad + g(\nu, w) - \frac{w}{2(\nu+1)} t(w|\nu+1) \\
&= -t(w|\nu+1) \frac{\alpha z \sqrt{\nu+1}}{2(\nu+z^2)^{3/2}} + \frac{1}{2} \left[-\psi \left(\frac{\nu+1}{2} \right) + \psi \left(\frac{\nu}{2} + 1 \right) \right] T(w|\nu+1) \\
&\quad + g(\nu, w)
\end{aligned} \tag{13}$$

where $g(\nu, w) := \int_{-\infty}^w \frac{1}{2} \log \left(\frac{\nu+1}{\nu+x^2+1} \right) t(x|\nu+1) dx$. Substituting Equation (13) into Equation (12), we

obtain

$$\begin{aligned} \frac{\partial \ell(\alpha, \nu)}{\partial \nu} &= \frac{1}{2} \log \left(\frac{\nu}{\nu + z^2} \right) - \frac{1}{2} \psi \left(\frac{\nu}{2} \right) + \frac{1}{2} \psi \left(\frac{\nu + 2}{2} \right) + \frac{z^2 - 1}{2(\nu + z^2)} \\ &\quad - h(w) \frac{\alpha z \sqrt{\nu + 1}}{2(\nu + z^2)^{3/2}} + \frac{g(\nu, w)}{T(w|\nu + 1)}, \end{aligned} \quad (14)$$

where $h(w) := t(w|\nu + 1)/T(w|\nu + 1)$. Next, we focus on the calculation of $g(\nu, w)$. Note that $\log \frac{\nu+1}{\nu+x^2+1}$ and $t(x|\nu + 1)$ are symmetric with respect to x , therefore for $w > 0$, we only consider

$$\begin{aligned} g_0(\nu, w) &= \int_0^w \frac{1}{2} \log \left(\frac{\nu + 1}{\nu + x^2 + 1} \right) t(x|\nu + 1) dx \\ &= \frac{1}{2} \int_0^w \log \left(\frac{\nu + 1}{\nu + x^2 + 1} \right) \frac{\left(\frac{\nu+1}{\nu+x^2+1} \right)^{\frac{\nu+2}{2}}}{\sqrt{\nu+1} B\left(\frac{\nu+1}{2}, \frac{1}{2}\right)} dx \\ &= \frac{1}{4} \int_0^{w^2} \frac{1}{\sqrt{u}} \log \left(\frac{\nu + 1}{\nu + u + 1} \right) \frac{\left(\frac{\nu+1}{\nu+u+1} \right)^{\frac{\nu+2}{2}}}{\sqrt{\nu+1} B\left(\frac{\nu+1}{2}, \frac{1}{2}\right)} du \\ &= \frac{1}{4B\left(\frac{\nu+1}{2}, \frac{1}{2}\right)} \int_{\frac{\nu+1}{\nu+w^2+1}}^1 \frac{y^{\frac{\nu-1}{2}}}{\sqrt{1-y}} \log(y) dy \\ &= + \frac{\sqrt{1+w^2+\nu}}{(1+\nu)^2} t(w|\nu + 1) {}_3F_2 \left(\frac{1}{2}, \frac{\nu}{2} + \frac{1}{2}, \frac{\nu}{2} + \frac{1}{2}; \frac{\nu}{2} + \frac{3}{2}, \frac{\nu}{2} + \frac{3}{2}; \frac{\nu+1}{\nu+w^2+1} \right) \\ &\quad - \frac{\sqrt{1+w^2+\nu}}{2(1+\nu)} \log \left(\frac{\nu+1}{\nu+w^2+1} \right) t(w|\nu + 1) {}_2F_1 \left(\frac{1}{2}, \frac{\nu+1}{2}; \frac{\nu+3}{2}; \frac{\nu+1}{\nu+w^2+1} \right) \\ &\quad - \frac{1}{4} \left[\psi \left(\frac{\nu}{2} + 1 \right) - \psi \left(\frac{\nu+1}{2} \right) \right]. \end{aligned} \quad (15)$$

Similarly, we have

$$g_1(\nu) = \int_0^{+\infty} \frac{1}{2} \log \left(\frac{\nu + 1}{\nu + x^2 + 1} \right) t(x|\nu + 1) dx = -\frac{1}{4} \left[\psi \left(\frac{\nu}{2} + 1 \right) - \psi \left(\frac{\nu+1}{2} \right) \right]. \quad (16)$$

Finally, we obtain $g(\nu, w)$ as follows:

$$g(\nu, w) = \begin{cases} g_0(\nu, w) + g_1(\nu) & \text{if } w \geq 0 \\ g_1(\nu) - g_0(\nu, w) & \text{otherwise.} \end{cases} \quad (17)$$

By take the partial derivative of Equation (14) with respect to α , we have

$$\frac{\partial^2 \ell(\alpha, \nu)}{\partial \nu \partial \alpha} = -\frac{\alpha z^2 (\nu + 1)}{2(\nu + z^2)^2} h'(w) - \frac{z \sqrt{\nu + 1}}{2(\nu + z^2)^{3/2}} h(w) + z h(w) \sqrt{\frac{\nu + 1}{\nu + z^2}} \left[\frac{1}{2} \log \left(\frac{\nu + 1}{\nu + w^2 + 1} \right) - \frac{g(\nu, w)}{T(w|\nu + 1)} \right], \quad (18)$$

where

$$h'(w) = -\frac{w(2+\nu)}{1+w^2+\nu} h(w) - h^2(w).$$

Because Equation (18) includes the terms with z^1 which is odd, therefore the Fisher Information of Equation (18) can be expressed as

$$I_{\alpha\nu} = -\mathbb{E} \left[h^2(w) \frac{\alpha z^2 (\nu + 1)}{2(\nu + z^2)^2} \right] + \mathbb{E} \left[z h(w) \sqrt{\frac{\nu + 1}{\nu + z^2}} \frac{g(\nu, w)}{T(w|\nu + 1)} \right] \quad (19)$$

By numeric results, we found that

$$\frac{g(\nu, w)}{T(w|\nu + 1)} = 2c_\nu * g_1(\nu),$$

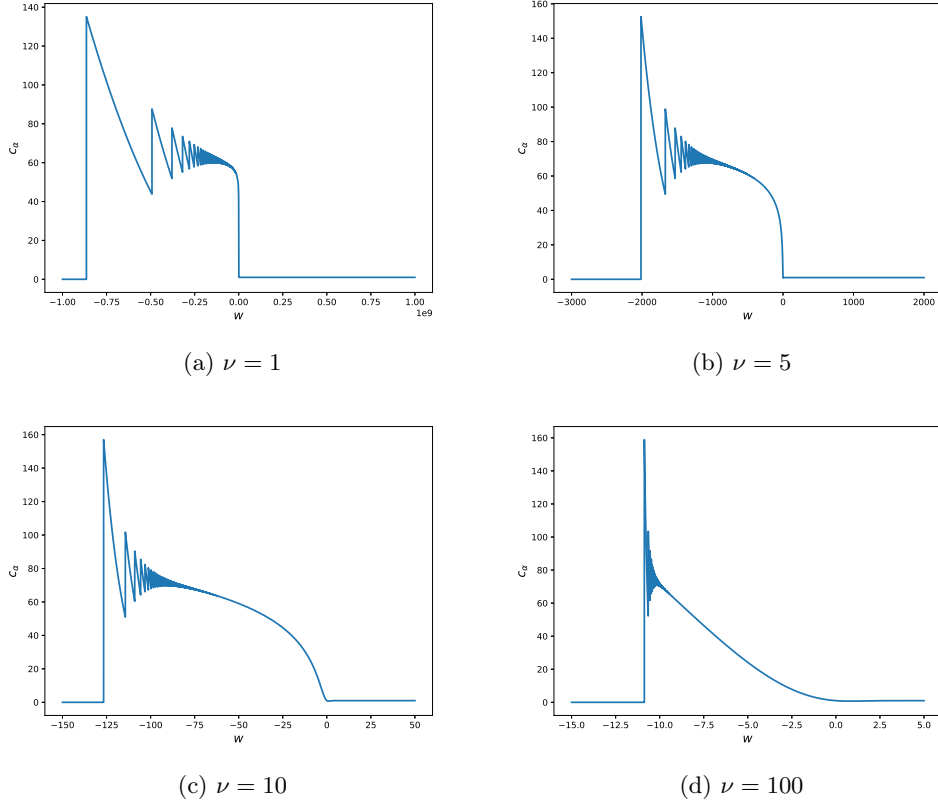


Figure 8: The c_ν for $\nu = 1, 5, 10, 100$. When $w \rightarrow -\infty$, $c_\nu \rightarrow 0$; When $w \rightarrow \infty$, $c_\nu \rightarrow 1$. Specially, if $w = 0$, $c_\nu = 1/2$. In the above figures, $c_\nu < 160$.

where c_ν is a constant only depending on ν , see [Figure 8](#). Therefore, [Equation \(19\)](#) can be written as

$$I_{\alpha\nu} = -\mathbb{E} \left[h^2(w) \frac{\alpha z^2 (\nu + 1)}{2(\nu + z^2)^2} \right],$$

and [Equation \(14\)](#) can be simplified as

$$\frac{\partial \ell(\alpha, \nu)}{\partial \nu} = \frac{1}{2} \log \left(\frac{\nu}{\nu + z^2} \right) + \frac{z^2 - 1}{2(\nu + z^2)} - h(w) \frac{\alpha z \sqrt{\nu + 1}}{2(\nu + z^2)^{3/2}} + d_\nu,$$

where $d_\nu := -\frac{1}{2} \psi \left(\frac{\nu}{2} \right) + \frac{1}{2} \psi \left(\frac{\nu+2}{2} \right) + 2c_\nu * g_1(\nu)$. Hence, the Fisher information with respect to ν can be expressed as

$$\begin{aligned} I_{\nu\nu} &= \mathbb{E} \left[\left(\frac{\partial \ell(\alpha, \nu)}{\partial \nu} \right)^2 \right] \\ &= \mathbb{E} \left[h^2(w) \frac{\alpha^2 z^2 (\nu + 1)}{4(\nu + z^2)^3} \right] + \frac{1}{4} \mathbb{E} \left[\left(\log \frac{\nu}{\nu + z^2} \right)^2 \right] + \frac{1}{4} \mathbb{E} \left[\left(\frac{z^2 - 1}{\nu + z^2} \right)^2 \right] + d_\nu^2 \\ &\quad + \frac{1}{2} \mathbb{E} \left[\left(\log \frac{\nu}{\nu + z^2} \right) \left(\frac{z^2 - 1}{\nu + z^2} \right) \right] + d_\nu \mathbb{E} \left[\log \frac{\nu}{\nu + z^2} \right] + d_\nu \mathbb{E} \left[\frac{z^2 - 1}{\nu + z^2} \right]. \end{aligned} \quad (20)$$

After some integrations, we obtain

$$\begin{aligned}
\mathbb{E} \left[\frac{z^2 - 1}{\nu + z^2} \right] &= 0 \\
\mathbb{E} \left[\log \frac{\nu}{\nu + z^2} \right] &= \psi \left(\frac{\nu}{2} \right) - \psi \left(\frac{\nu + 1}{2} \right) \\
\mathbb{E} \left[\left(\log \frac{\nu}{\nu + z^2} \right) \left(\frac{z^2 - 1}{\nu + z^2} \right) \right] &= -\frac{1}{\nu^2 + \nu} \\
\mathbb{E} \left[\left(\frac{z^2 - 1}{\nu + z^2} \right)^2 \right] &= \frac{1}{\nu^2 + 3\nu} \\
\mathbb{E} \left[\left(\log \frac{\nu}{\nu + z^2} \right)^2 \right] &= \left(\psi \left(\frac{\nu}{2} \right) - \psi \left(\frac{\nu + 1}{2} \right) \right)^2 + \psi^{(1)} \left(\frac{\nu}{2} \right) - \psi^{(1)} \left(\frac{\nu + 1}{2} \right) \\
\mathbb{E} \left[h^2(w) \frac{\alpha^2 z^2 (\nu + 1)}{4(\nu + z^2)^3} \right] &= \frac{\pi^{5/2} \Gamma \left(\frac{\nu}{2} + 1 \right) ((\nu + 3)H_1 - (\nu + 3)H_2 - H_3 + H_4)}{8\nu^2 \Gamma \left(\frac{\nu+5}{2} \right) B \left(\frac{\nu}{2}, \frac{1}{2} \right) B \left(\frac{\nu+1}{2}, \frac{1}{2} \right)^2} \\
\mathbb{E} \left[h^2(w) \frac{\alpha z^2 (\nu + 1)}{2(\nu + z^2)^2} \right] &= \frac{\pi \alpha \Gamma \left(\frac{\nu}{2} + 1 \right)^2 \left((\nu + 4)H_5 - \frac{(\alpha^2(2\nu+3) + (\nu+3)\sigma_{\nu+1}^2)H_6}{\sigma_{\nu+1}^2} \right)}{8(\alpha^2 + \sigma_{\nu+1}^2) \Gamma \left(\frac{\nu+1}{2} \right) \Gamma \left(\frac{\nu+5}{2} \right)},
\end{aligned}$$

where

$$\begin{aligned}
H_1 &= {}_2F_1 \left(\frac{1}{2}, \nu + 1; \frac{\nu + 3}{2}; -\frac{\alpha^2}{\sigma_{\nu+1}^2} \right) \\
H_2 &= {}_2F_1 \left(\frac{1}{2}, \nu + 2; \frac{\nu + 3}{2}; -\frac{\alpha^2}{\sigma_{\nu+1}^2} \right) \\
H_3 &= {}_2F_1 \left(\frac{3}{2}, \nu + 1; \frac{\nu + 5}{2}; -\frac{\alpha^2}{\sigma_{\nu+1}^2} \right) \\
H_4 &= {}_2F_1 \left(\frac{3}{2}, \nu + 2; \frac{\nu + 5}{2}; -\frac{\alpha^2}{\sigma_{\nu+1}^2} \right) \\
H_5 &= {}_2F_1 \left(-\frac{1}{2}, \nu + 2; \frac{\nu + 5}{2}; -\frac{\alpha^2}{\sigma_{\nu+1}^2} \right) \\
H_6 &= {}_2F_1 \left(\frac{1}{2}, \nu + 2; \frac{\nu + 5}{2}; -\frac{\alpha^2}{\sigma_{\nu+1}^2} \right),
\end{aligned}$$

which completes the proof. □

Other results in [Section 3.2](#)

	n	z	t	CG	AD	BIGPAST
FPR	50	0.0874	0.0788	0.0788	0.2214	0.0473
	100	0.0677	0.0630	0.0630	0.1920	0.0389
	200	0.0595	0.0571	0.0571	0.1972	0.0223
	400	0.0533	0.0520	0.0520	0.1870	0.0144
TPR	50	0.9631	0.9574	0.9574	0.8090	0.9190
	100	0.9820	0.9802	0.9802	0.8393	0.9571
	200	0.9974	0.9968	0.9968	0.8586	0.9790
	400	0.9983	0.9982	0.9982	0.8564	0.9819
ACC	50	0.9379	0.9393	0.9393	0.7938	0.9359
	100	0.9572	0.9586	0.9586	0.8237	0.9591
	200	0.9689	0.9698	0.9698	0.8307	0.9784
	400	0.9725	0.9731	0.9731	0.8347	0.9837

Table 6: The simulation results of false positive rate (FPR), true positive rate (TPR) and accuracy (ACC), derived from single-subject observations that consist of 50% positive and 50% negative, are presented under the assumption that the direction of alternative hypothesis is ‘less’. Each cell in the resulting table is calculated based on one million test outcomes. ‘CG’ and ‘AD’ represent the Crawford-Garthwaite Bayesian and Anderson-Darling methods, respectively.

	n	z	t	CG	AD	BIGPAST
FPR	50	0.0003	0.0002	0.0002	0.4511	0.0030
	100	0.0000	0.0000	0.0000	0.4654	0.0044
	200	0.0000	0.0000	0.0000	0.4699	0.0027
	400	0.0000	0.0000	0.0000	0.4701	0.0021
TPR	50	0.6402	0.5907	0.5908	0.8229	0.8858
	100	0.5445	0.5197	0.5198	0.7792	0.9206
	200	0.5824	0.5693	0.5694	0.8491	0.9628
	400	0.5389	0.5323	0.5323	0.8197	0.9670
ACC	50	0.8199	0.7953	0.7953	0.6859	0.9414
	100	0.7722	0.7599	0.7599	0.6569	0.9581
	200	0.7912	0.7847	0.7847	0.6896	0.9800
	400	0.7694	0.7661	0.7661	0.6748	0.9825

Table 7: The simulation results of false positive rate (FPR), true positive rate (TPR) and accuracy (ACC), derived from single-subject observations that consist of 50% positive and 50% negative, are presented under the assumption that the direction of alternative hypothesis is ‘greater’. Each cell in the resulting table is calculated based on one million test outcomes. ‘CG’ and ‘AD’ represent the Crawford-Garthwaite Bayesian and Anderson-Darling methods, respectively.

	n	z	t	CG	AD	BIGPAST
FPR	50	0.0467	0.0322	0.0322	0.0943	0.0313
	100	0.0372	0.0286	0.0286	0.0523	0.0266
	200	0.0324	0.0280	0.0280	0.0541	0.0231
	400	0.0243	0.0220	0.0220	0.0392	0.0195
TPR	50	0.9353	0.9041	0.9041	0.9125	0.8854
	100	0.9504	0.9358	0.9359	0.9302	0.9248
	200	0.9617	0.9542	0.9541	0.9621	0.9450
	400	0.9737	0.9700	0.9700	0.9568	0.9596
ACC	50	0.9443	0.9360	0.9359	0.9091	0.9270
	100	0.9566	0.9536	0.9536	0.9389	0.9491
	200	0.9647	0.9631	0.9631	0.9540	0.9610
	400	0.9747	0.9740	0.9740	0.9588	0.9701

Table 8: The simulation results of false positive rate (FPR), true positive rate (TPR) and accuracy (ACC), derived from single-subject observations that consist of 50% positive and 50% negative, are presented under the assumption that the direction of alternative hypothesis is ‘two-sided’. The underlying density is normal density function. Each cell in the resulting table is calculated based on one million test outcomes. ‘CG’ and ‘AD’ represent the Crawford-Garthwaite Bayesian and Anderson-Darling methods, respectively.

Other results in Section 3.3

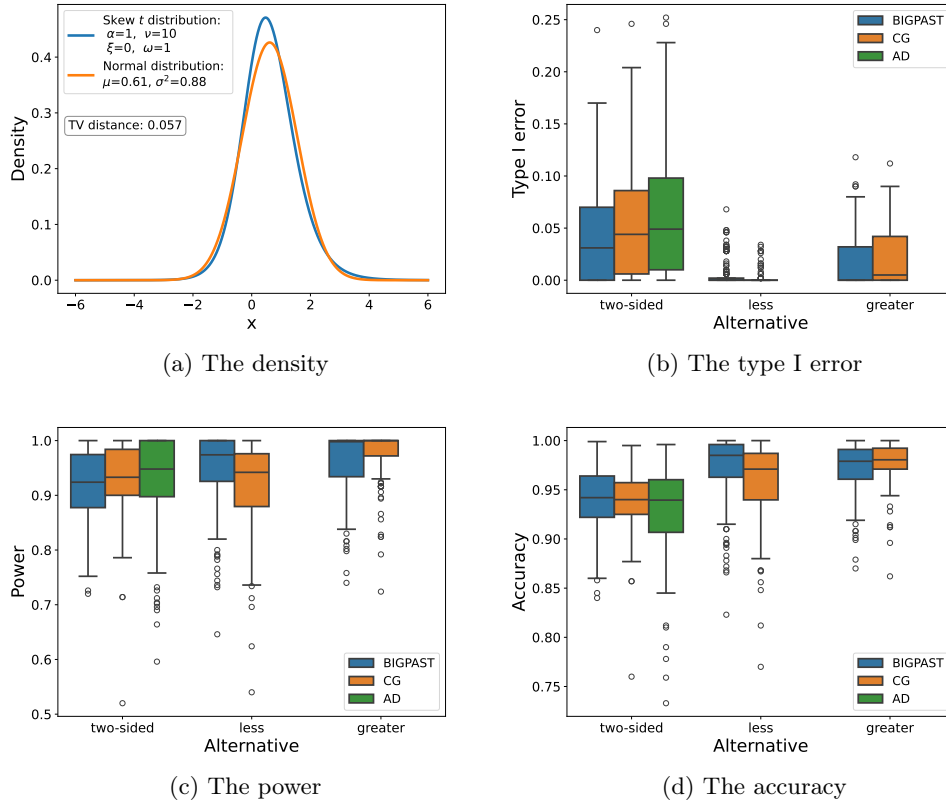
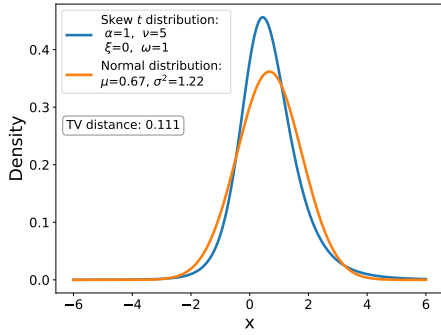
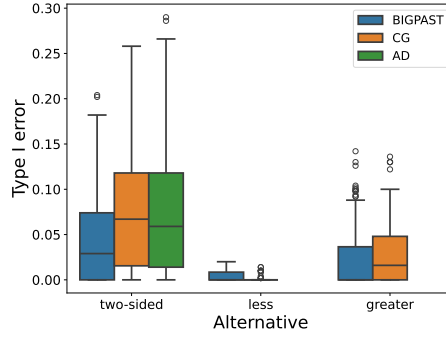


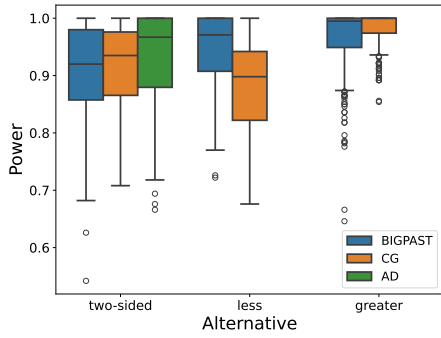
Figure 9: The comparison results of BIGPAST, CG and AD approaches under three alternative hypotheses: ‘two-sided’, ‘less’ and ‘greater’ respectively when $\alpha = 1$ and $\nu = 10$. Figure 9a shows the densities of skewed Student’s t and normal distributions, the μ and σ^2 of normal distribution are equal to the mean and variance of skewed Student’s t distribution. In fact, the normal distribution is the theoretical assumption of CG test when the sample comes from the skewed Student’s t distribution. AD test is a nonparametric test; there is one result that is compared in the ‘two-sided’ category. TV distance is short for total variation distance. Each box plot summarises over 200 independent replications.



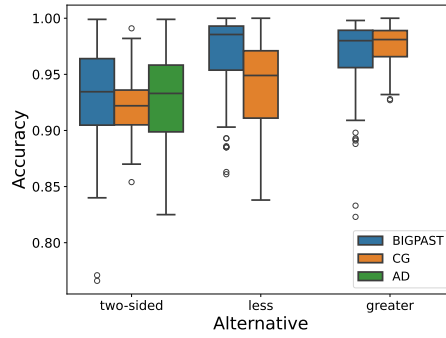
(a) The density



(b) The type I error



(c) The power



(d) The accuracy

Figure 10: The comparison results of BIGPAST, CG and AD approaches under three alternative hypotheses: ‘two-sided’, ‘less’ and ‘greater’ respectively when $\alpha = 1$ and $\nu = 5$. Figure 10a shows the densities of skewed Student’s t and normal distributions, the μ and σ^2 of normal distribution are equal to the mean and variance of skewed Student’s t distribution. In fact, the normal distribution is the theoretical assumption of CG test when the sample comes from the skewed Student’s t distribution. AD test is a nonparametric test; there is one result that is compared in the ‘two-sided’ category. TV distance is short for total variation distance. Each box plot summarises over 200 independent replications.

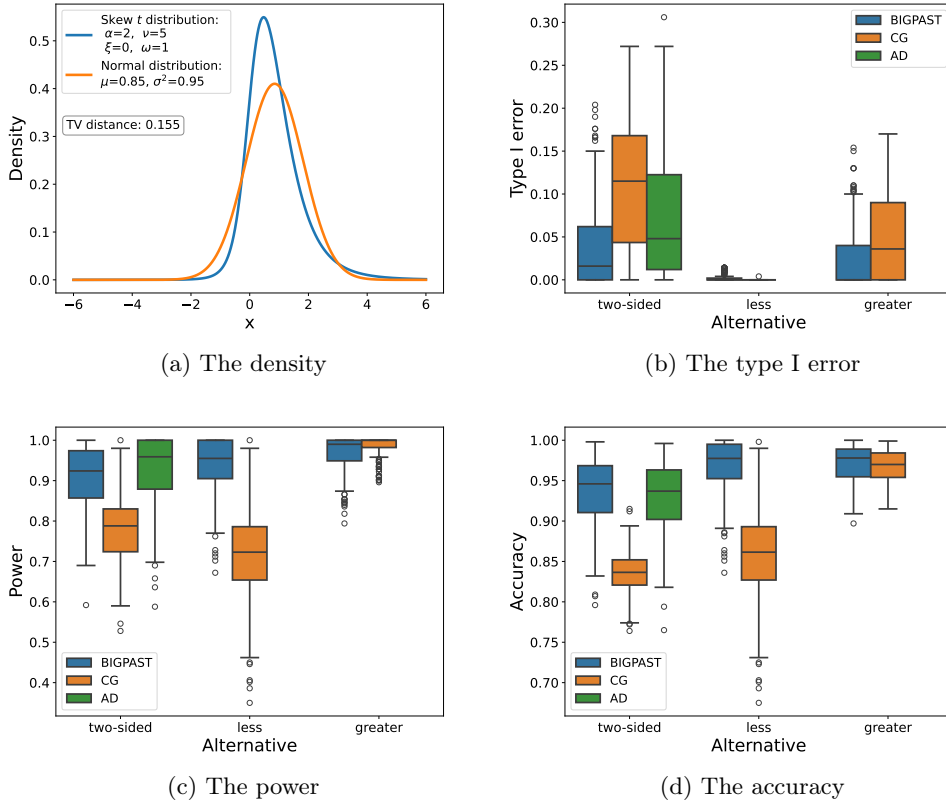


Figure 11: The comparison results of BIGPAST, CG and AD approaches under three alternative hypotheses: 'two-sided', 'less' and 'greater' respectively when $\alpha = 2$ and $\nu = 5$. Figure 11a shows the densities of skewed Student's t and normal distributions, the μ and σ^2 of normal distribution are equal to the mean and variance of skewed Student's t distribution. In fact, the normal distribution is the theoretical assumption of the CG test when the sample comes from the skewed Student's t distribution. AD test is a nonparametric test; there is one result that is compared in the 'two-sided' category. TV distance is short for total variation distance. Each box plot summarises over 200 independent replications.

Index	label_name	Index	label_name
0	lh-bankssts	34	rh-bankssts
1	lh-caudalanteriorcingulate	35	rh-caudalanteriorcingulate
2	lh-caudalmiddlefrontal	36	rh-caudalmiddlefrontal
3	lh-cuneus	37	rh-cuneus
4	lh-entorhinal	38	rh-entorhinal
5	lh-frontalpole	39	rh-frontalpole
6	lh-fusiform	40	rh-fusiform
7	lh-inferiorparietal	41	rh-inferiorparietal
8	lh-inferiortemporal	42	rh-inferiortemporal
9	lh-insula	43	rh-insula
10	lh-isthmuscingulate	44	rh-isthmuscingulate
11	lh-lateraloccipital	45	rh-lateraloccipital
12	lh-lateralorbitofrontal	46	rh-lateralorbitofrontal
13	lh-lingual	47	rh-lingual
14	lh-medialorbitofrontal	48	rh-medialorbitofrontal
15	lh-middletemporal	49	rh-middletemporal
16	lh-paracentral	50	rh-paracentral
17	lh-parahippocampal	51	rh-parahippocampal
18	lh-parsopercularis	52	rh-parsopercularis
19	lh-parsorbitalis	53	rh-parsorbitalis
20	lh-parstriangularis	54	rh-parstriangularis
21	lh-pericalcarine	55	rh-pericalcarine
22	lh-postcentral	56	rh-postcentral
23	lh-posteriorcingulate	57	rh-posteriorcingulate
24	lh-precentral	58	rh-precentral
25	lh-precuneus	59	rh-precuneus
26	lh-rostralanteriorcingulate	60	rh-rostralanteriorcingulate
27	lh-rostralmiddlefrontal	61	rh-rostralmiddlefrontal
28	lh-superiorfrontal	62	rh-superiorfrontal
29	lh-superiorparietal	63	rh-superiorparietal
30	lh-superiortemporal	64	rh-superiortemporal
31	lh-supramarginal	65	rh-supramarginal
32	lh-temporalpole	66	rh-temporalpole
33	lh-transversetemporal	67	rh-transversetemporal

Table 9: The index of brain region of the Desikan-Killiany cortical atlas.